ATLAS upgrade material
*by **Anna Duncan***
BOOST 2017

Upgrades & Expected DM Performance at the HL-LHC

Julie Hogan, on behalf of the CMS collaboration

Brown University

Dark Matter Workshop – July 27, 2017

HL-LHC UPGRADES

- Huge fluences expected in HL-LHC conditions
- Expect ~300/fb in Run2 and then ~3000/fb over the course of the HL-LHC – upgraded detectors have to last through it!
- Pileup conditions will kill many current algorithms
- Many CMS and ATLAS subsystems need extensive rebuilds

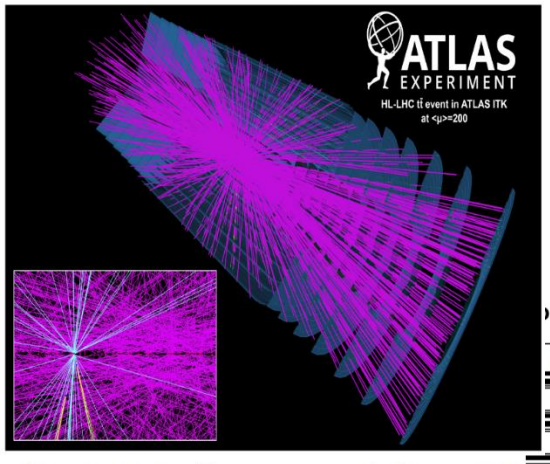

Simulated $t\bar{t}$ event at $\langle\mu\rangle = 200$

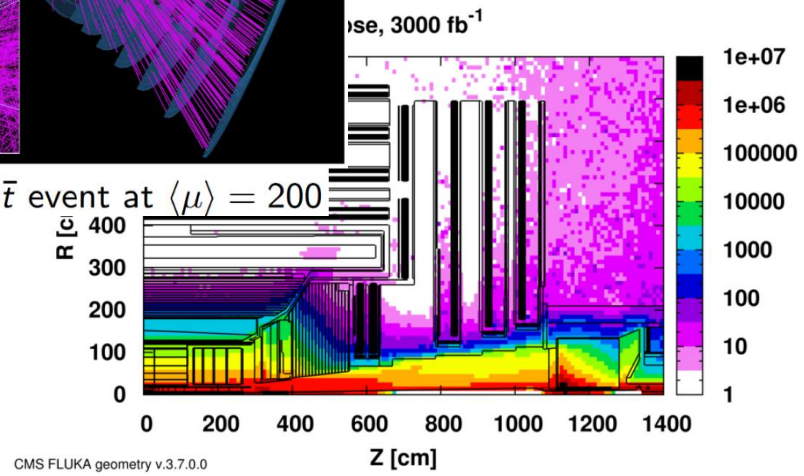

Benchmark:
Up to 7.5 x 10^{34} /cm^2 or 200 PU

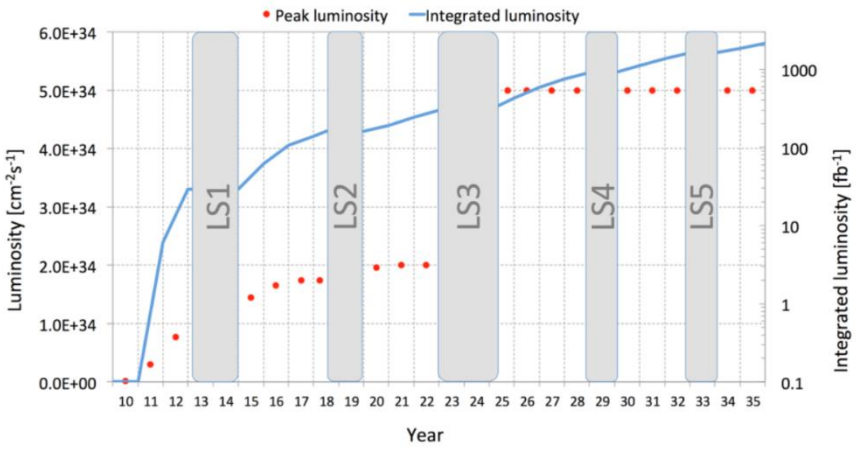

CMS HL-LHC UPGRADES

Trigger/HLT/DAQ
- Track information in hardware event selection
- 750 kHz hardware event selection
- 7.5 kHz events registered

Barrel EM calorimeter
- New electronics
- Low operating temperature ≈ -10◦

Muon systems
- New DT & CSC electronics
- New chambers $1.6 < \eta < 2.4$
- Muon tagging $2.4 < \eta < 3$

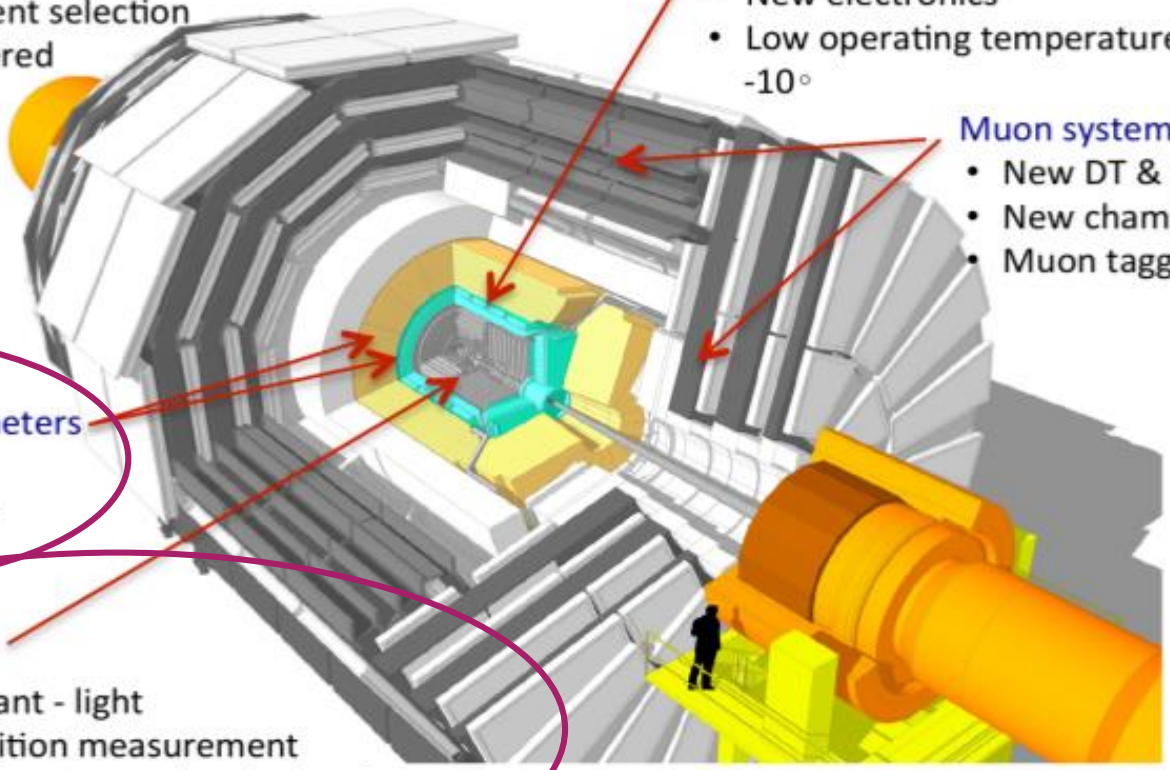

New Endcap Calorimeters
- Rad. Tolerant
- 5D measurement

New Tracker
- Rad. Tolerant - light
- High Definition measurement
- 40 MHz selective readout for hardware trigger
- Extended Pixel coverage to $\eta \approx 3.8$

Beam radiation and luminosity
Common systems and infrastructure

LHC: New low-b triplet quadropoles + crab cavities

CMS TRACKING UPGRADES

- Radiation tolerance: blue = dead @ 1000/fb
- Higher granularity for lower occupancy
- Increased coverage, pixels out to $|\eta| \sim 4$
- Better track separation, reduce hit merging in high energy jets
- Reduced material

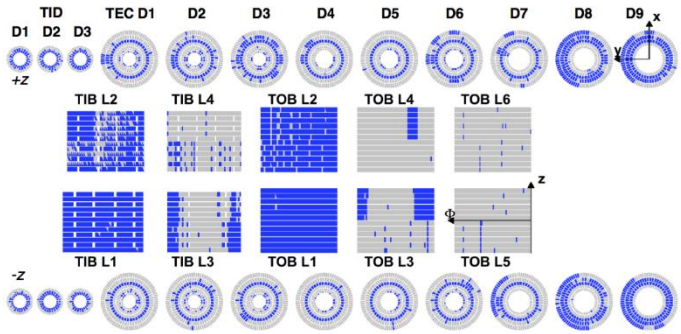

CMS TP

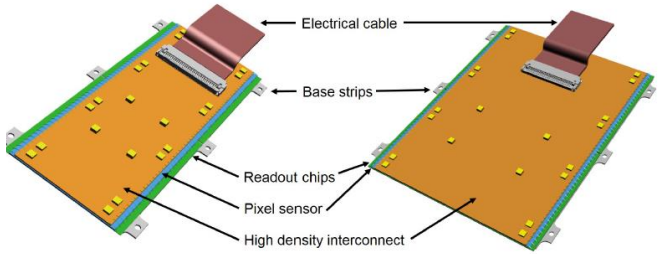

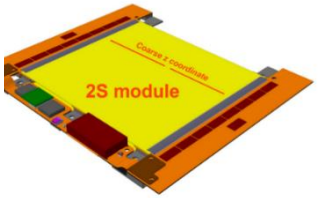

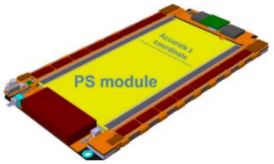

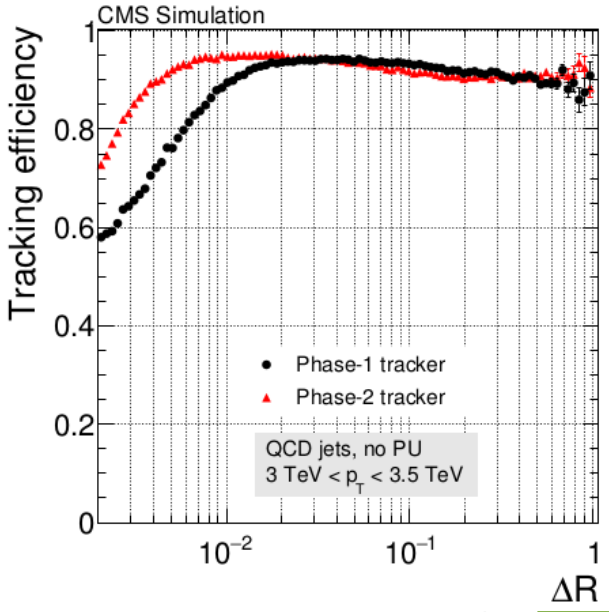

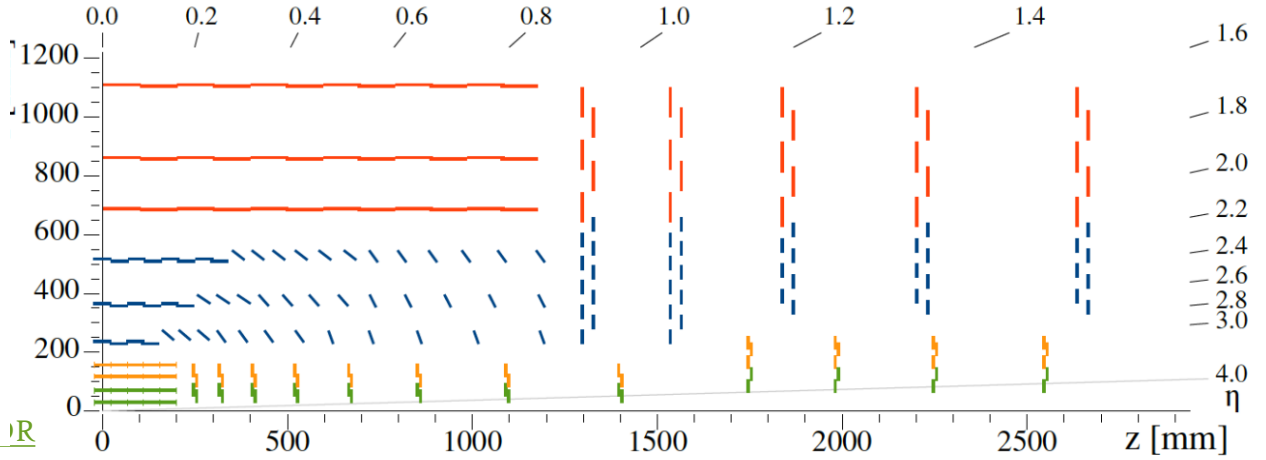

CMS TRACKING UPGRADES

- Efficient track finding for L-1 trigger
- Stub-finding in 2-sensor modules
- 15k stubs @ 14 MHz, p_T > 2 GeV
- Goal is FPGA-only tracking

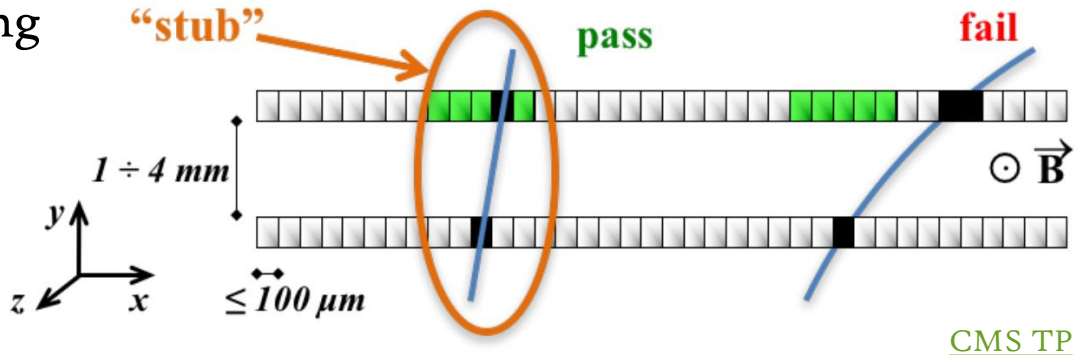

CMS TP

FPGA tracklet (stub-pair) road search tracking

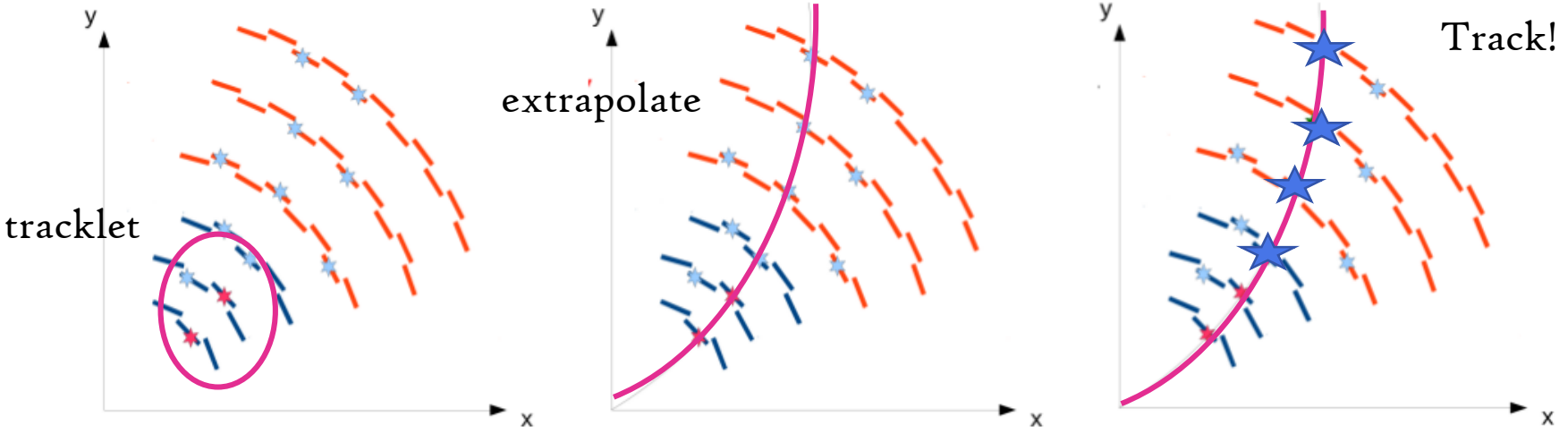

CMS VERTEXING PERFORMANCE

- Merging vertices become an issue as pileup and density increase
- Vertexing efficiency drops with pileup density
- Motivates timing detector upgrade – use both time and space to select vertices

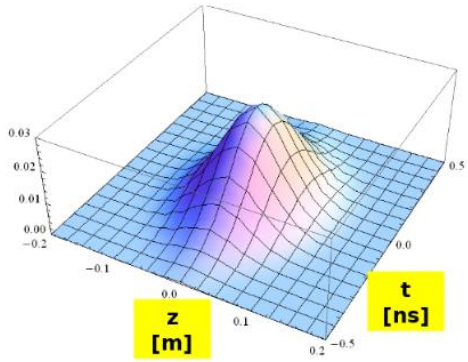

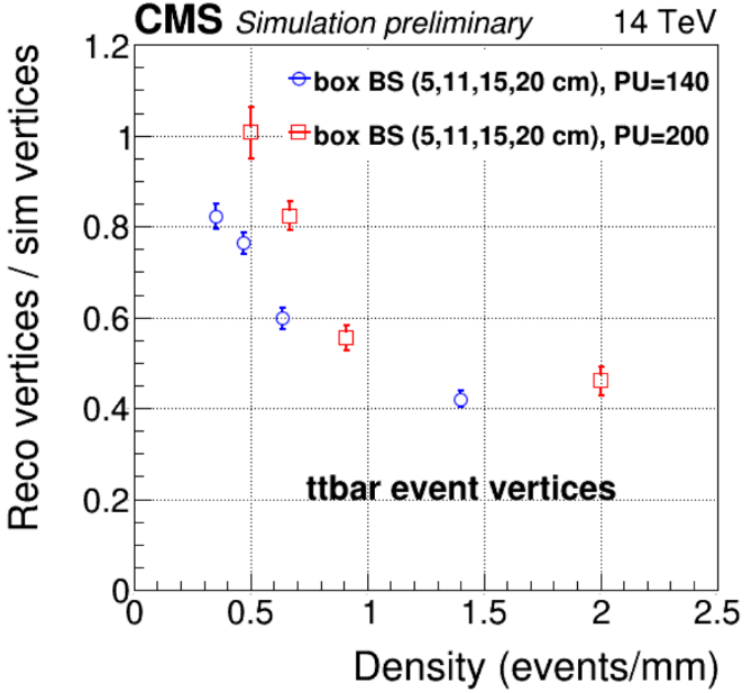

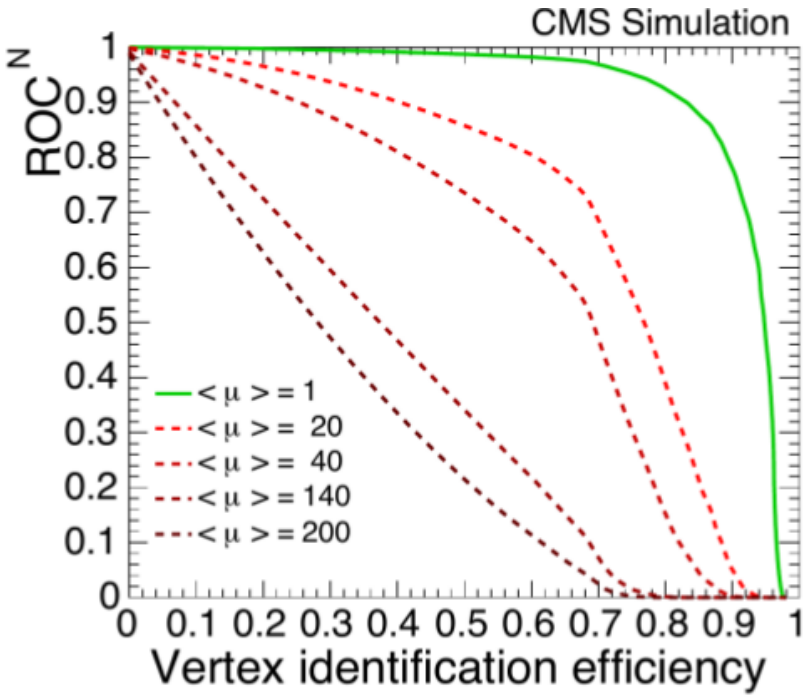

CMS MIP TIMING LAYER

- MIP timing layer now part of upgrade plan, TDR this fall
- Separate vertices in time as well as space for 4D reconstruction
- Significant reduction of pileup tracks associated to the PV

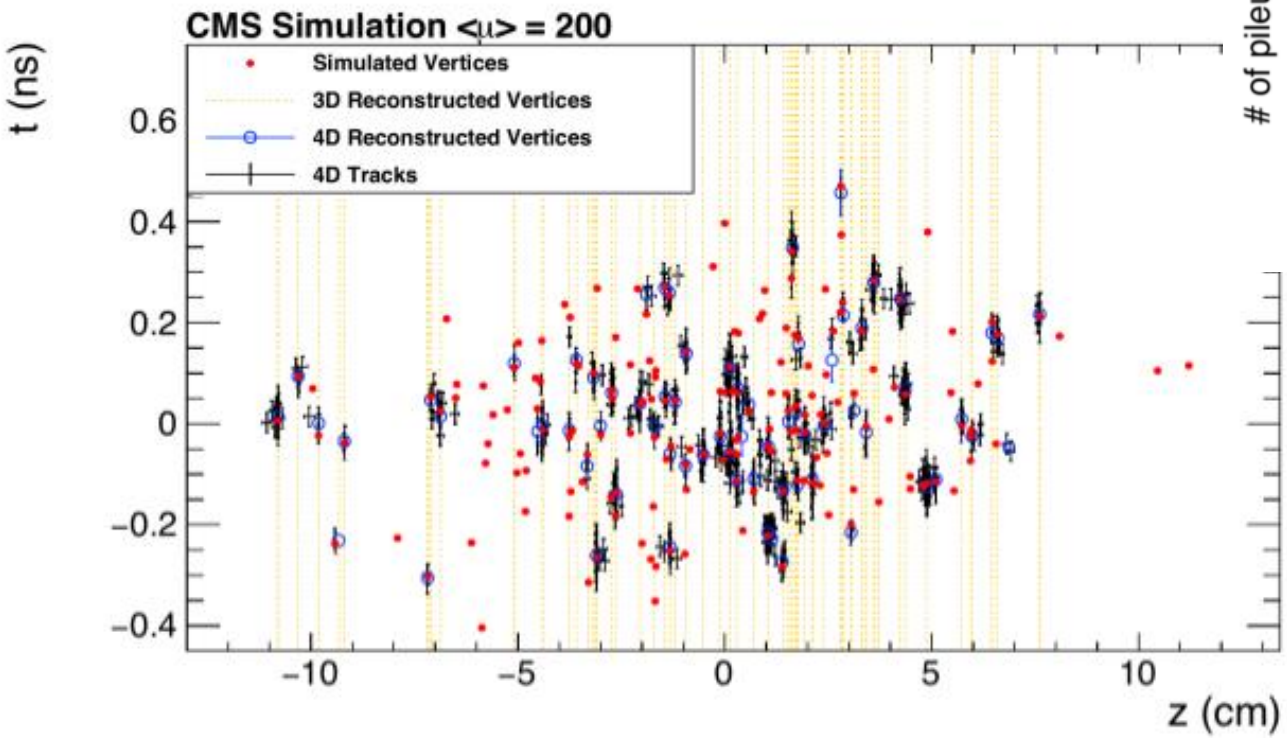

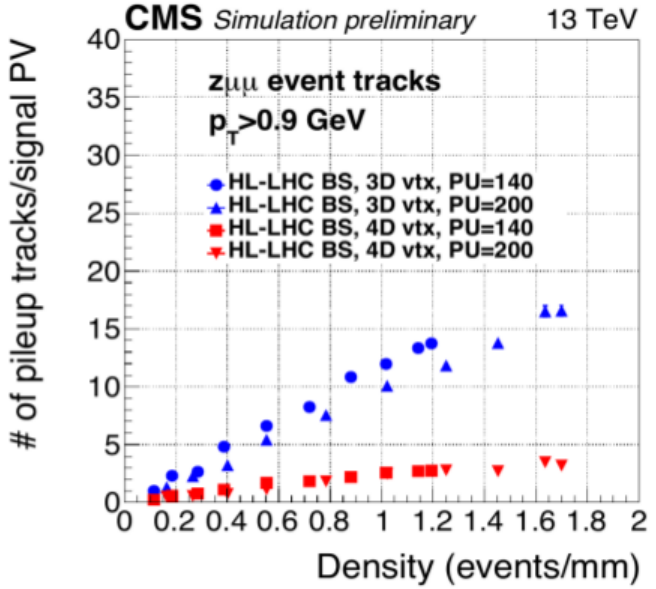

Multiple blue circles on a vertical yellow line indicate vertices that would be merged without timing layer

20ps charge hadron res.

CMS CALORIMETRY UPGRADES

- **High granularity silicon endcap calorimeter – 3D shower images**
  - EM endcap: tungsten/copper plates + silicon sensors
  - Front hadronic endcap: brass/copper plates + silicon sensors
  - Backing hadronic endcap: brass + plastic scintillator
  - Hexagonal sensors cooled to -30 C to minimize damage

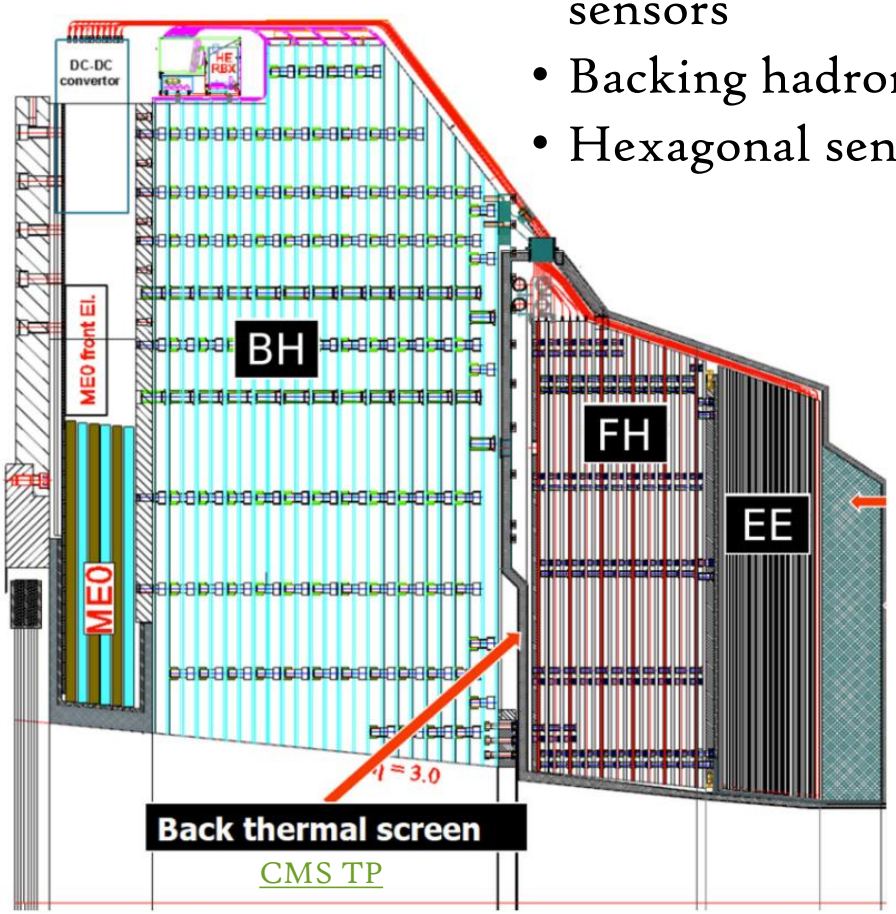

CMS TP

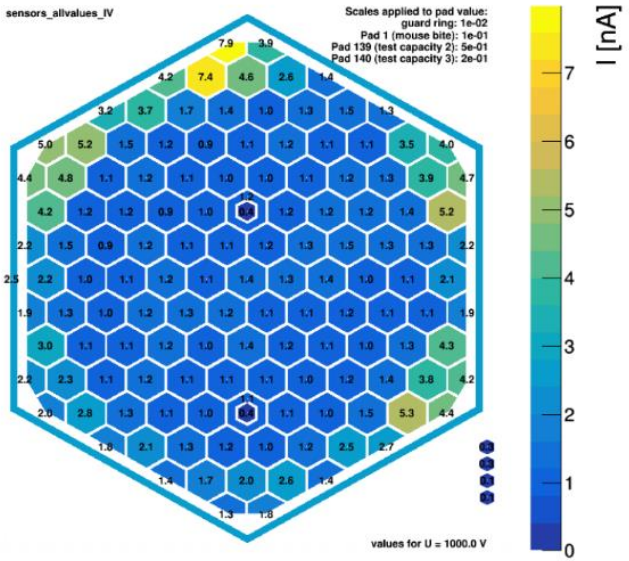

HPK 6" p-on-n 128 channel sensors
I_{leak} @ 1000V: average for 15 sensors

CMS JET PERFORMANCE

- **PUPPI performs strongly for HL-LHC**
  - Smaller corrections than PF jets
  - Isolation for muons more performant than PF-based isolation with the same cone
  - Resolution < 20% for p_T > 40
- B-tagging now possible out to $|\eta|$ = 3.5
  - Current performance can be maintained up to 140 pileup

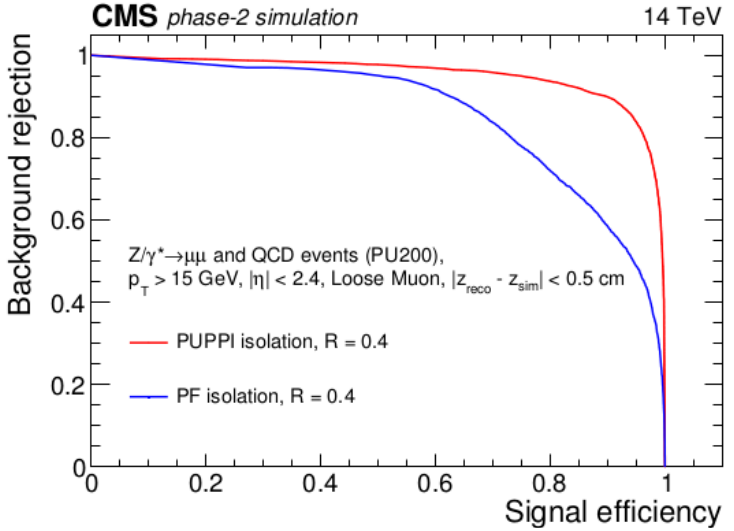

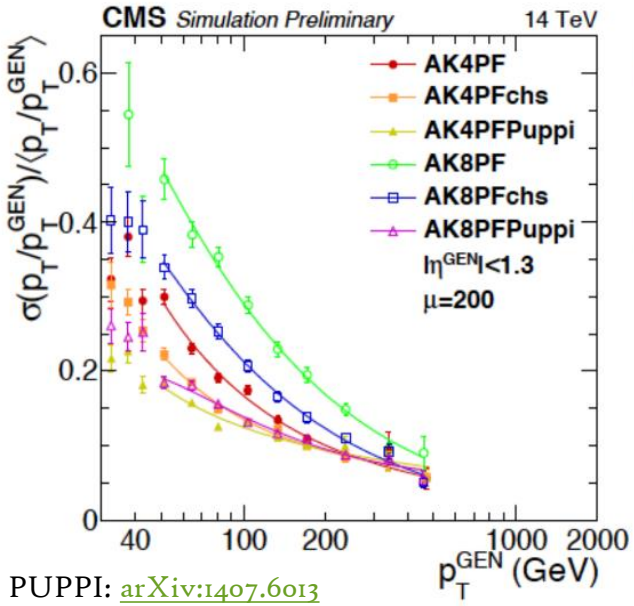

PUPPI: arXiv:1407.6013

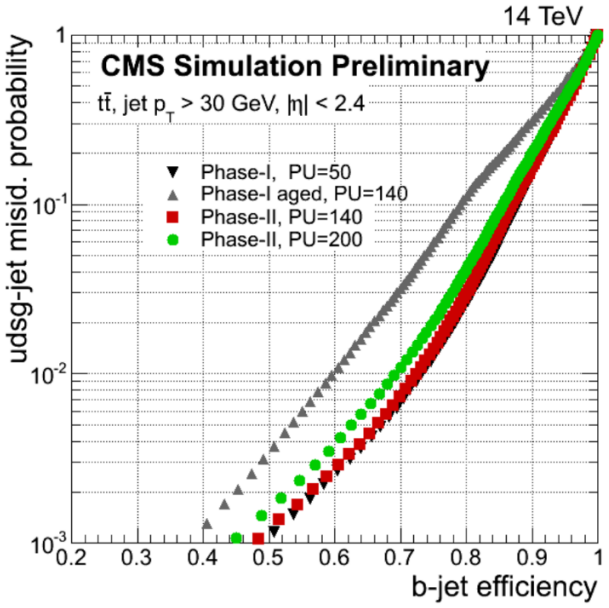

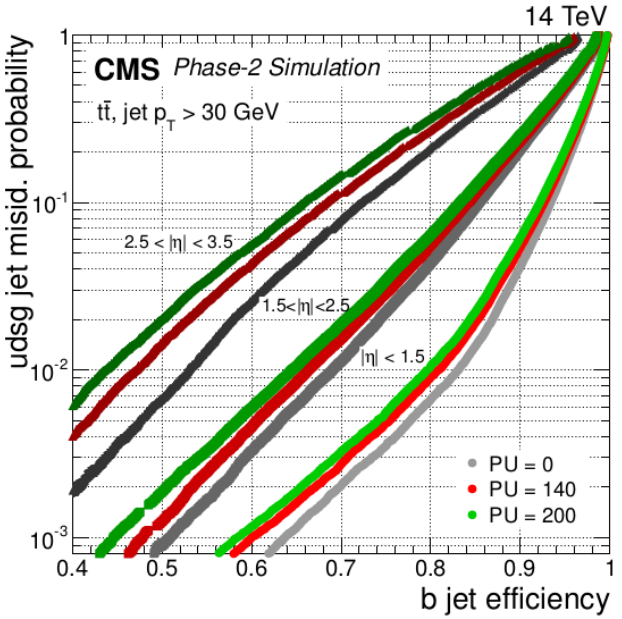

CMS JET PERFORMANCE

- PUPPI MET resolutions show a clear benefit from the tracker extension and limited degradation between 140 and 200 pileup
- Timing layer + PUPPI jets from upgraded calorimetry reproduces the energy spectrum from no-pileup simulations in 140 pileup

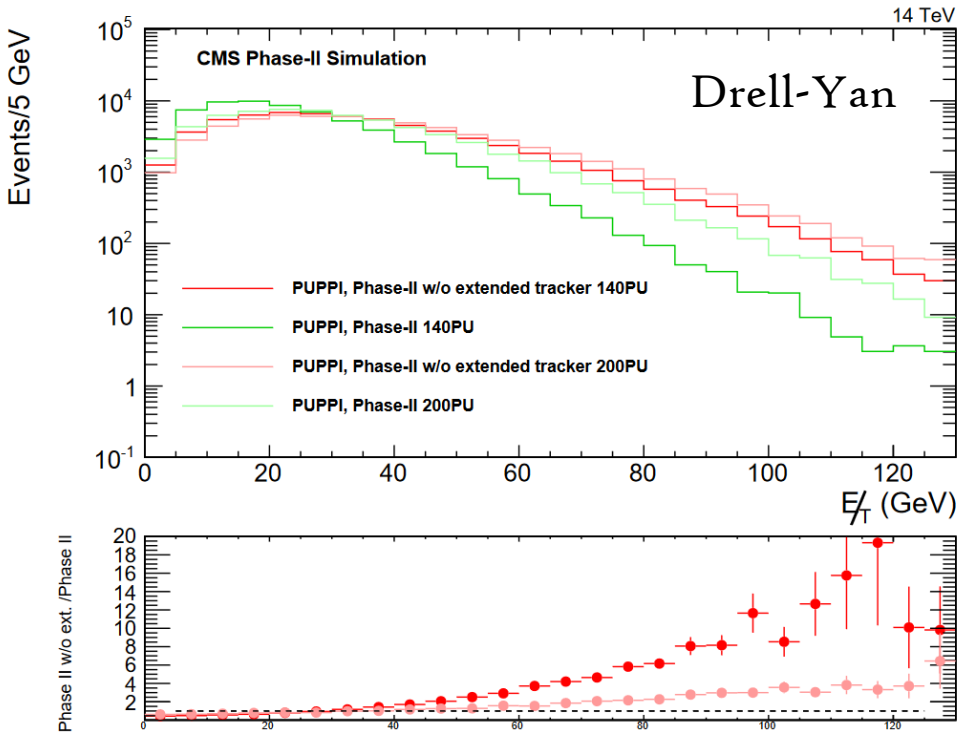

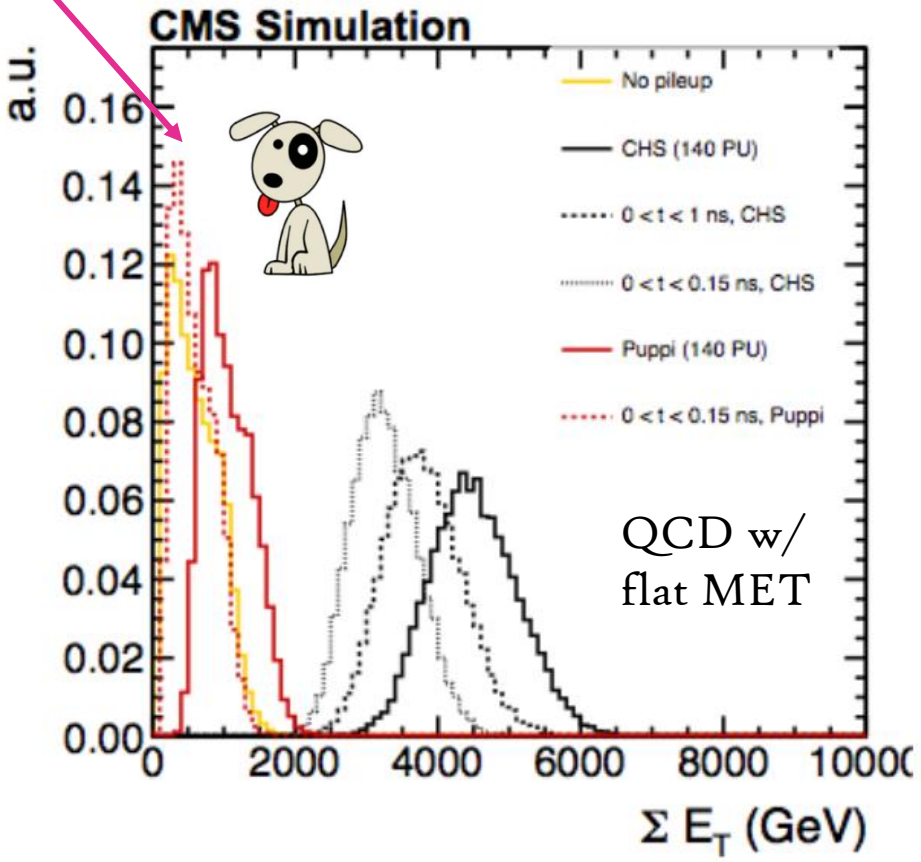

ATLAS HL-LHC UPGRADES

- Silicon trackers: pixels surrounded by strips
  - Higher granularity to reduce occupancy
  - Reduced material in front of calorimeters
  - Extended coverage ($\eta < 4.0$)
  - Provides tracking information to L1 trigger
- New trigger/DAQ architecture to cope with increased data rates
- Proposed: High Granularity Forward Timing Detector ($2.4 < |\eta| < 4.2$)
- New electronics for calorimeters
- Modified muon detector

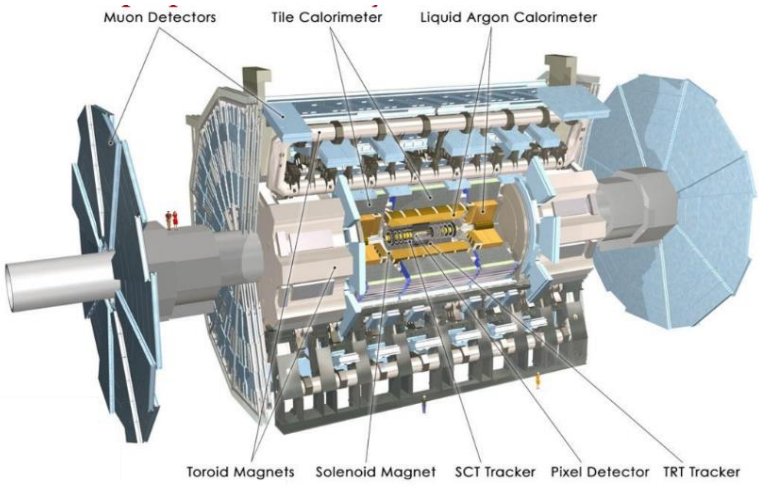

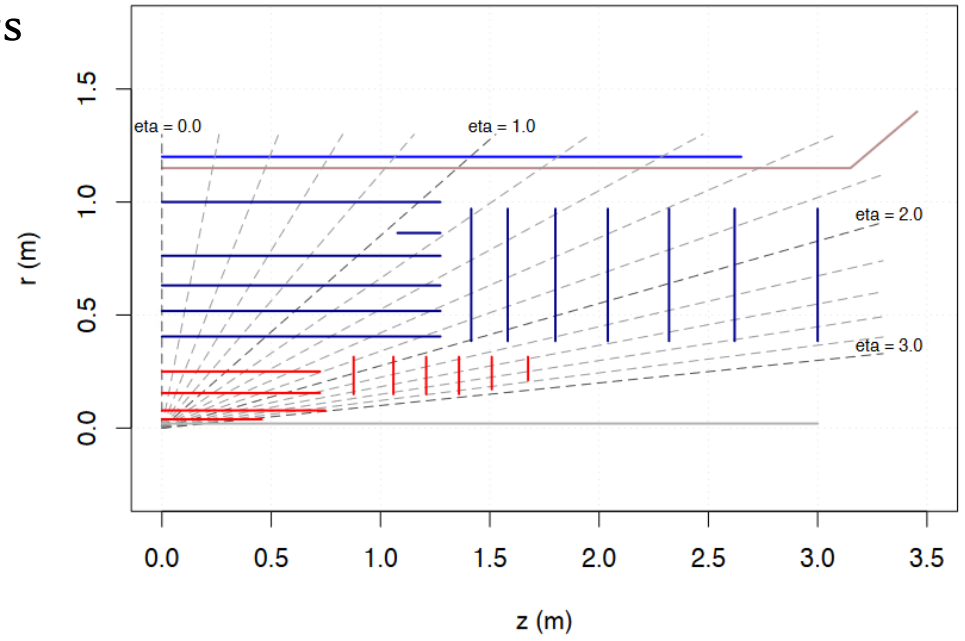

ATLAS TIMING DETECTOR

- High granularity timing detector in the forward region
- With track timing to 30ps, 50% of pileup tracks can be removed from the hard scatter vertices
- Combined with inner tracker allows pileup-jet rejection close to truth-level performance

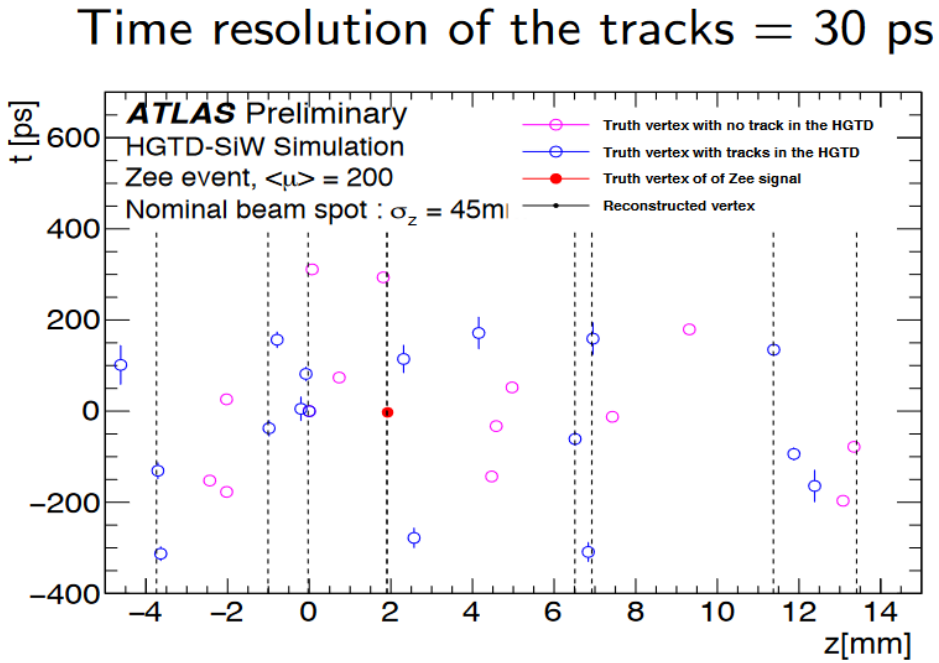

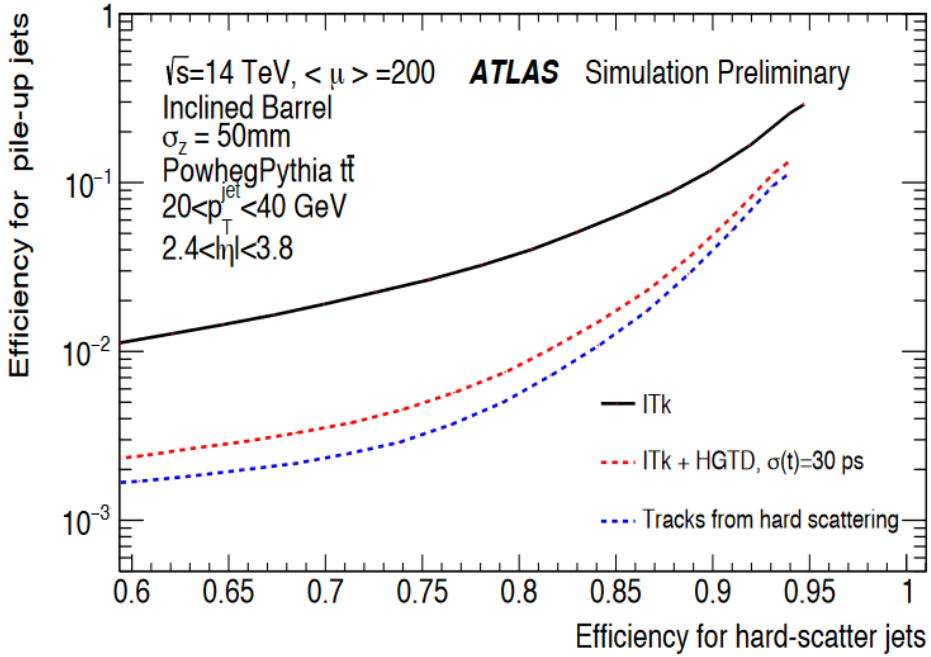

ATLAS JET PERFORMANCE

- Extended eta coverage benefits pileup mitigation – jet vertex tagger can be extended to the forward region
- Standard methods based on PV association of tracks within jets

HS/ PU jet discriminator: $R_{p_T} = \frac{\Sigma_k p_T^{trk_k}(PV_0)}{p_T^{jet}}$

$E_T^{miss} = \Sigma \text{high } p_T \text{ objects} + \text{soft term}$

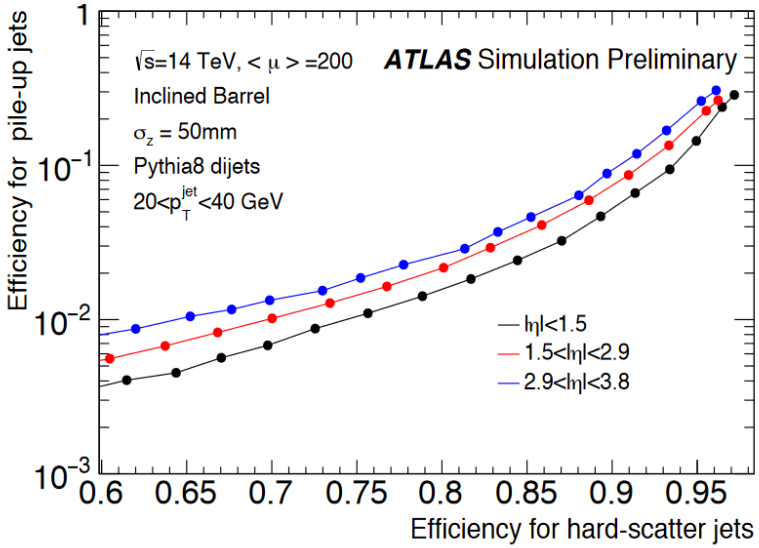

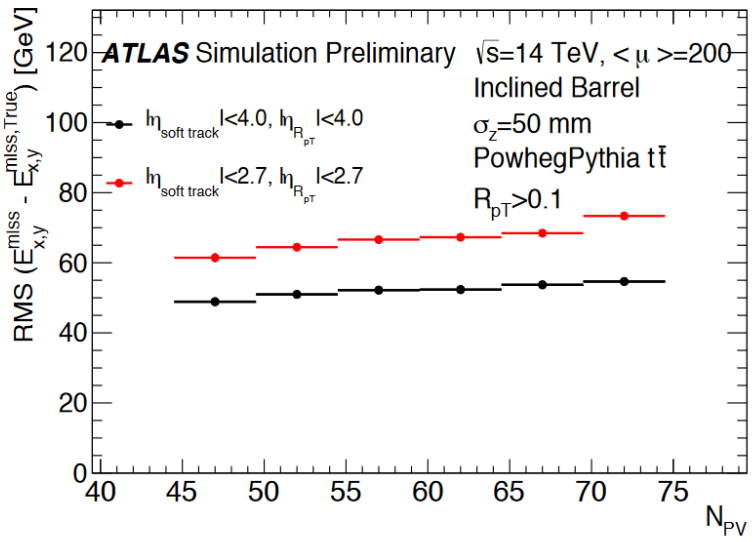

Higher fake rate in forward region due to more pile-up tracks associated to HS.

Soft term from charged tracks assigned to HS vertex $\Longrightarrow$ forward pile-up rejection essential for good E_T^{miss} reconstruction.

ATLAS JET PERFORMANCE

- At high pileup, Voronoi and constituent subtraction used for pileup mitigation, extending jet area corrections
- "SoftKiller" removes soft particles with a dynamic threshold
- "Cluster Vertex Fraction" extends jet-vertex-tagger to consituents

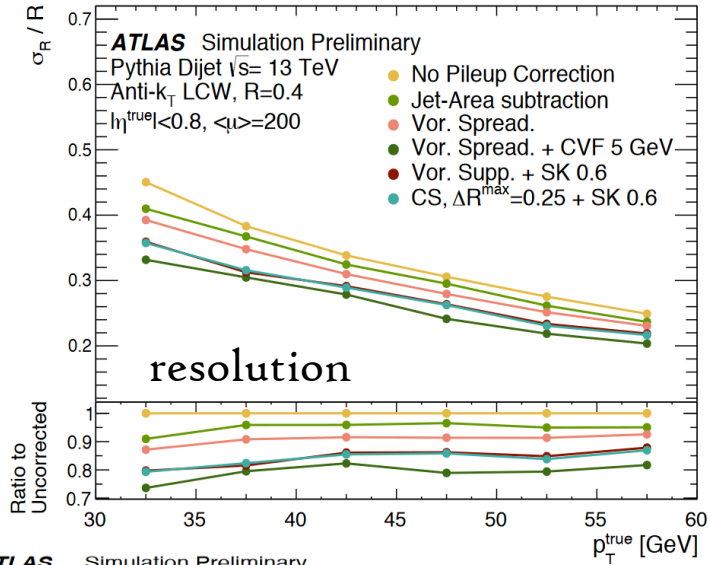

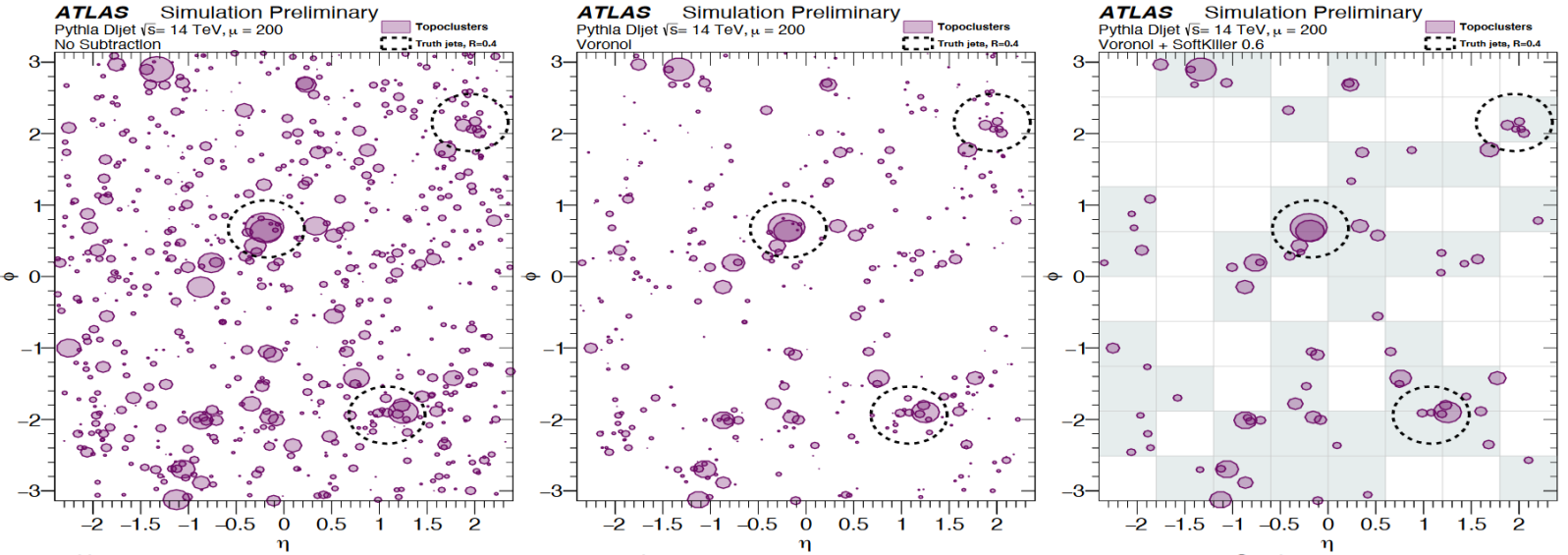

No sub → Voronai → + SoftKiller

Efficient pileup removal vs removal of hard scatter clusters ⟹ optimise SoftKiller grid size

ATLAS JET PERFORMANCE

- Proof of performance for pileup mitigation techniques for retaining mass resolution of large-R jets
- Trimming applied on R=1.0 jets with or without jet area corrections
- Track-assisted mass improves resolution:

$$m_{TA} = \frac{p_T^{calo}}{p_T^{track}} \times m^{track}$$

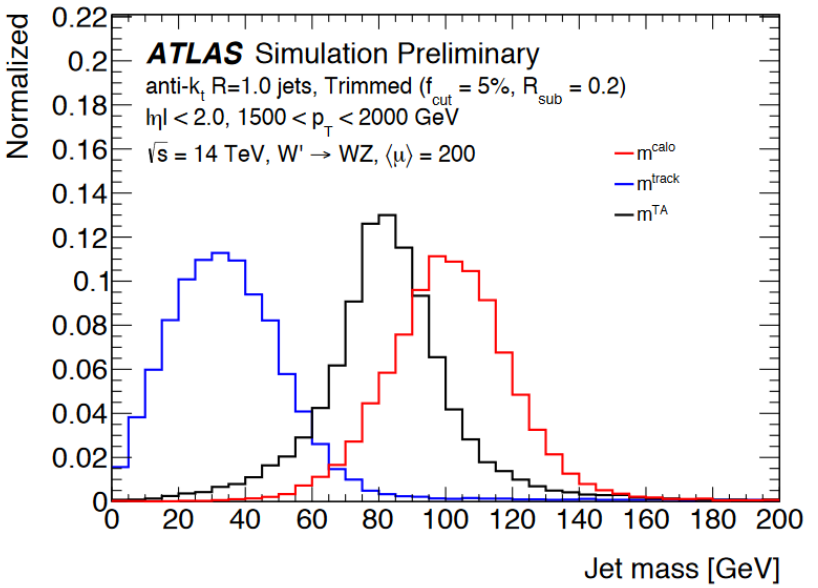

no suppression

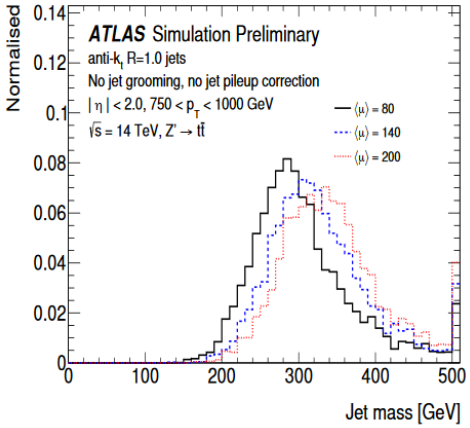

jet area correction

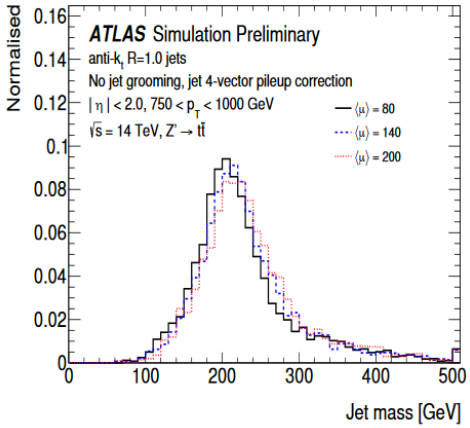

jet trimming

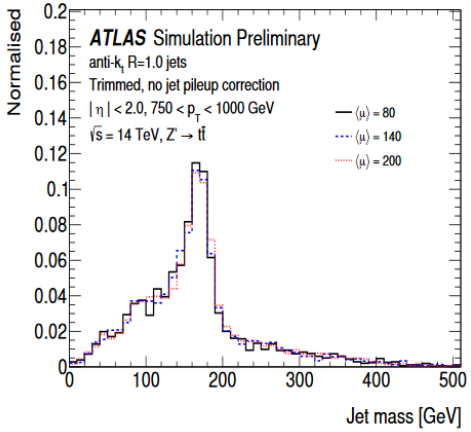

combination

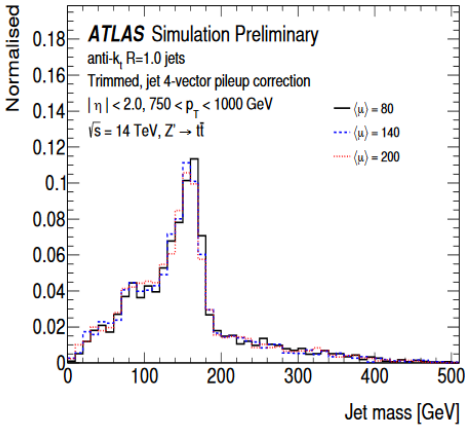

PHYSICS SENSITIVITY

- Several current boosted topology searches have been projected forward into HL-LHC scenarios, with varying assumptions about improvements in systematic uncertainties
- CMS Monojet dark matter search

EXO-16-037

  - Axial vector mediator: MET extended to > 2.4 TeV, consider equal or reduced 2x/4x MET uncerts.
  - Pseudo-scalar mediator: same MET range, consider equal or lumi-scaled MET uncertainties

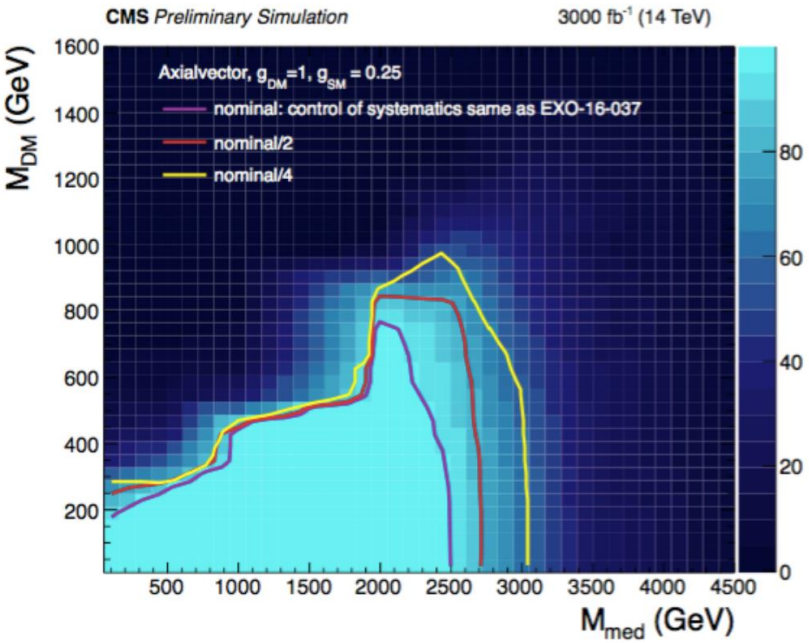

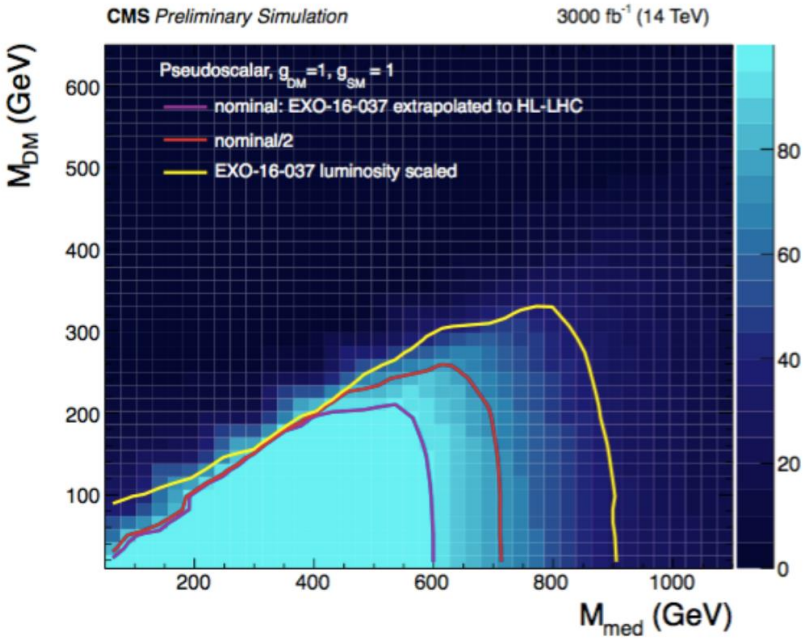

PHYSICS SENSITIVITY

- ATLAS monojet dark matter
- Jet momentum > 300 GeV, MET > 400, 600, 800 GeV
- Lower limits on suppression scale mass out to ~3 TeV, dependent on what systematic uncertainties can be obtained

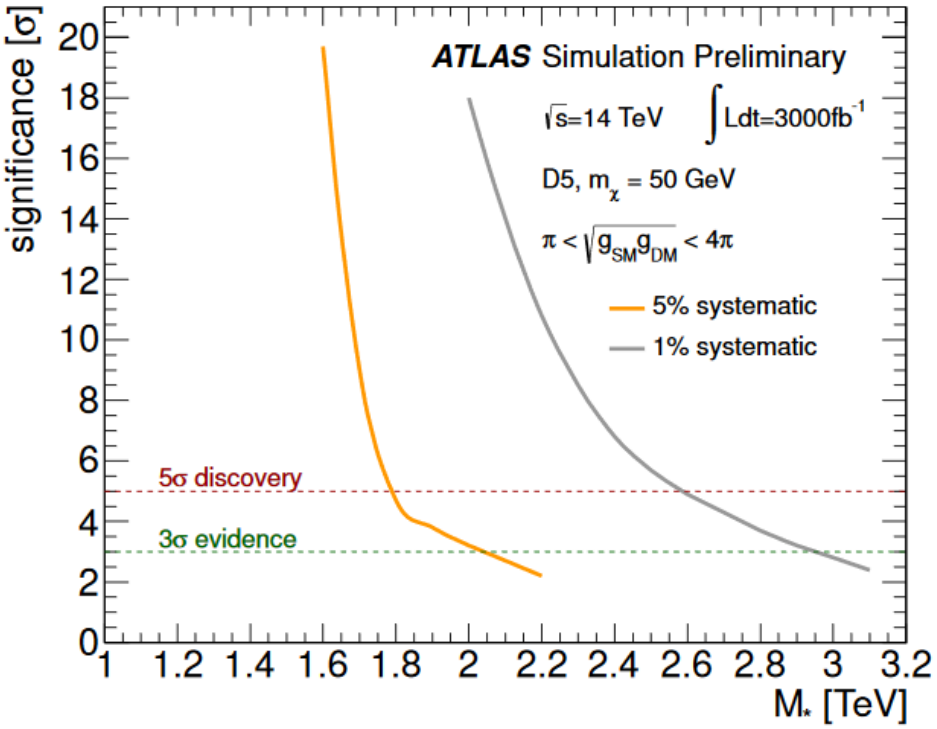

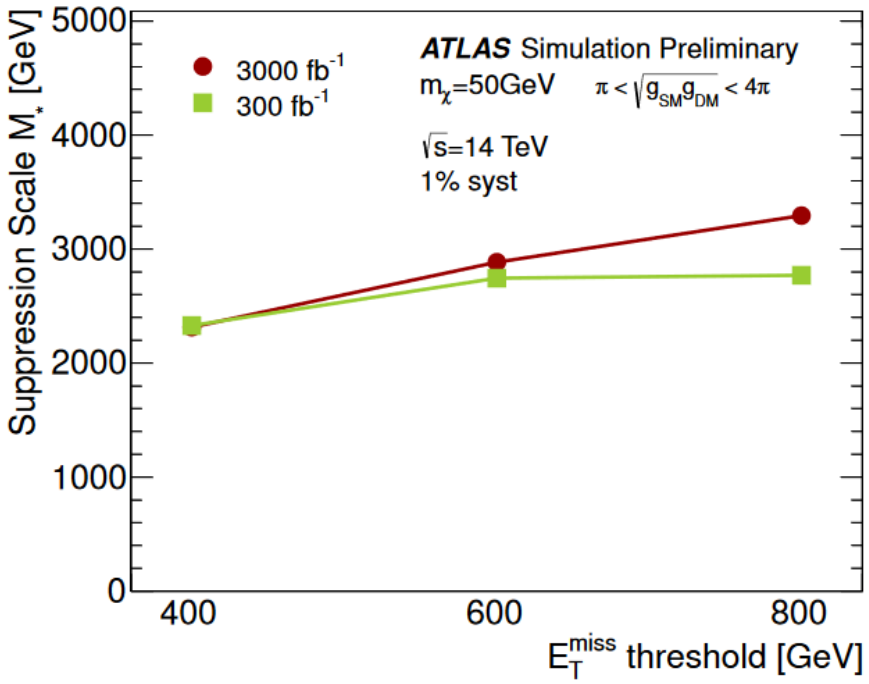

SUMMARY

- Upgrade programs are progressing well with dedicated efforts in both collaborations
- Performance studies make a clear case for the importance of the upgrades, and plans are in place for multiple funding scenarios
- Active area of work – exciting new challenges for design and reconstruction where new technological and computing developments could make a big effect
- We'll be ready when HL-LHC is here!

CMS links
Technical Proposal
Scope Document
Timing, Object, Physics Notes
Tracker Technical Design Report

ATLAS links
Letter of Intent
Scope Document
Dark Matter Projection
More in Anna's BOOST talk

BACKUP

TRACKER MODULES

- Two pixel options: rectangular 25 x 100 microns or 50 x 50 microns
- Both effective after high fluence, rectangular currently preferred
- Also investigating 3D innermost layer option

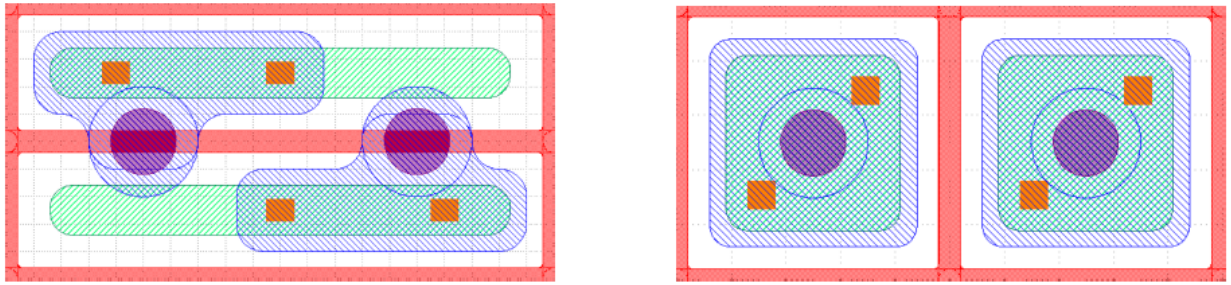

Figure 4.6: Drawing of two adjacent pixel cells for sensors from the HPK submission with pixel size $25 \times 100\ \mu m^2$ (left) and $50 \times 50\ \mu m^2$ (right). The n^+ implants are shown in green, the metal layers in blue, the p-stop areas in red, the contacts in orange, and the bump bond pads in purple.

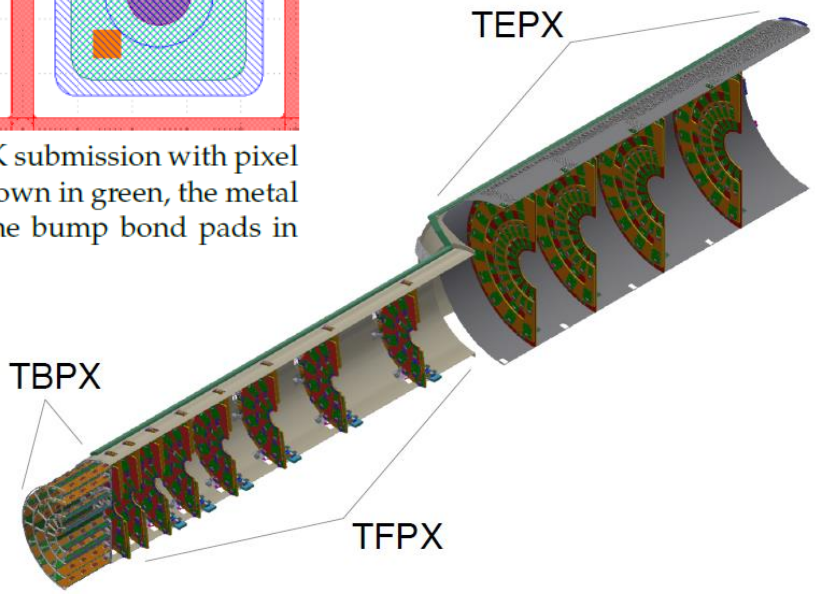

Figure 4.2: Perspective view of one quarter of the Inner Tracker, showing the TBPX ladders and TFPX and TEPX dees inside the supporting structures. The pixel modules are shown as orange elements in TBPX and as green elements in TFPX and TBPX. The dees are depicted as red and orange surfaces.

TRACKER MODULES

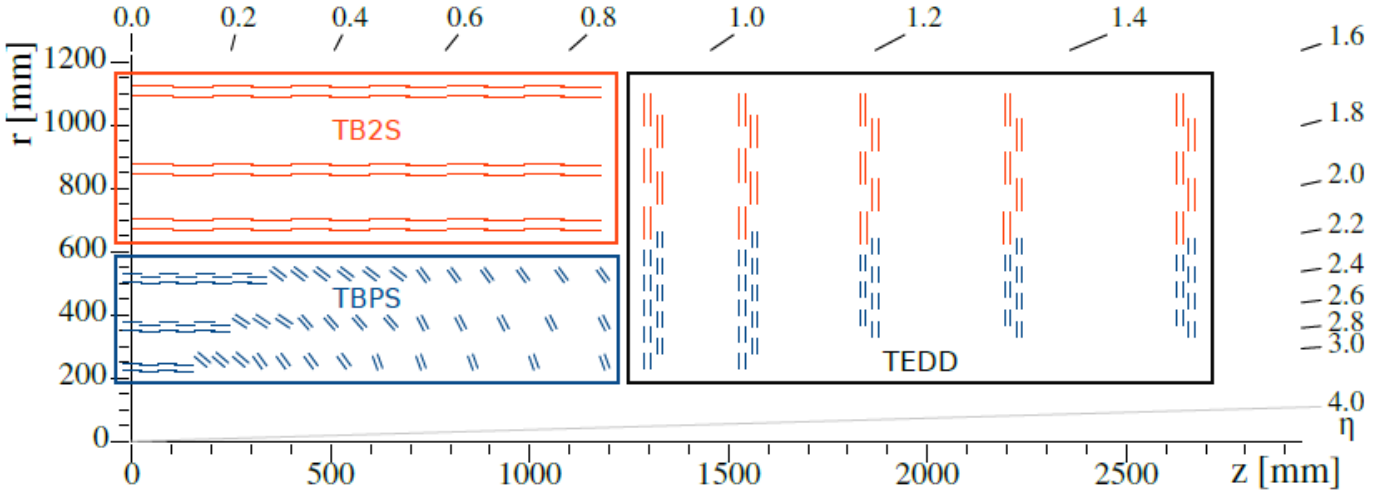

Figure 3.1: Sketch of one quarter of the Outer Tracker in *r*-*z* view. Blue (red) lines represent PS (2S) modules. The three sub-detectors, named TBPS, TB2S, and TEDD, are indicated. All overlapping layers are shown separately, while in Fig. 2.3 the mean positions are shown.

Table 3.3: Dimensions and quantities of the three sensor types used in the Outer Tracker. All dimensions are given in micrometres. The active area is defined as the area enclosed within the centre line between the outermost strip implant or pixel implant and the bias ring implant. At this transition approximately half of the charge generated by a particle is lost to the bias ring. The percentage of spares is larger for the PS-p sensors as compared to the strip sensors, as the PS-p sensors will undergo bump bonding.

Sensor	Outer		Active		Strip/Pixel		Quantity	Quantity
name	width	length	width	length	pitch	length	needed	with spares
2S	94 183	102 700	91 440	100 548	90	50 274	15 360	17 660 (+15%)
PS-s	98 140	49 160	96 000	46 944	100	23 472	5 616	6 460 (+15%)
PS-p	98 740	49 160	96 000	46 944	100	1 467	5 616	6 740 (+20%)

TRACKING PERFORMANCE

- Compared to current detector, momentum and impact parameter resolutions will dramatically improve
- Use ttbar events as a tracking benchmark
  - Efficiency fairly stable with pileup
  - Fakerates increase with pileup

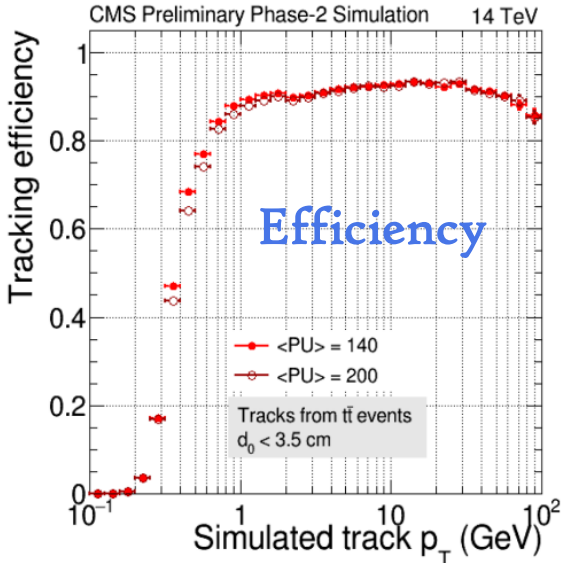

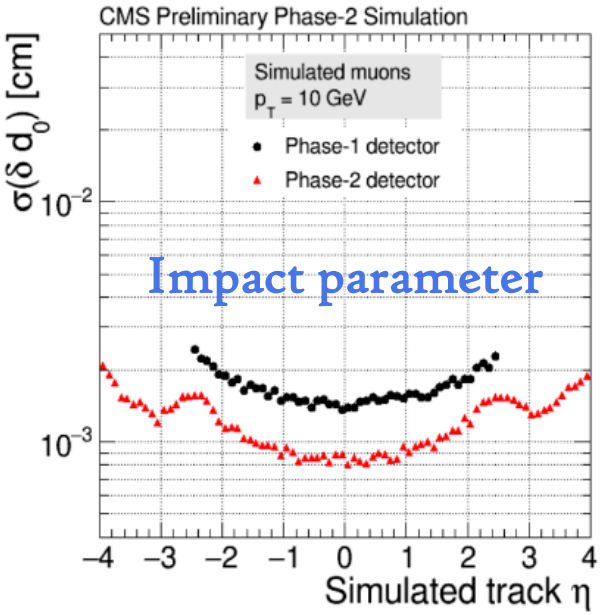

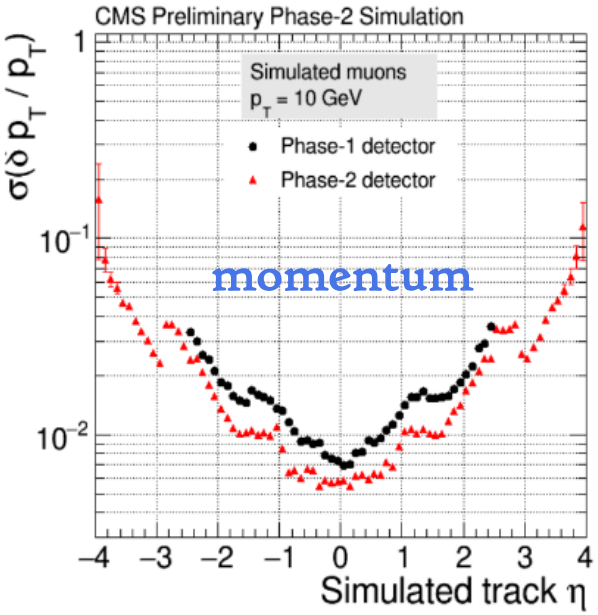

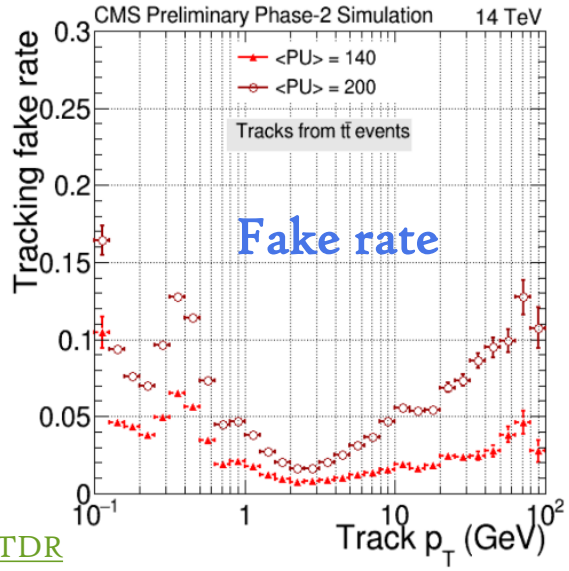

Trk TDR

TRACKER MODULES

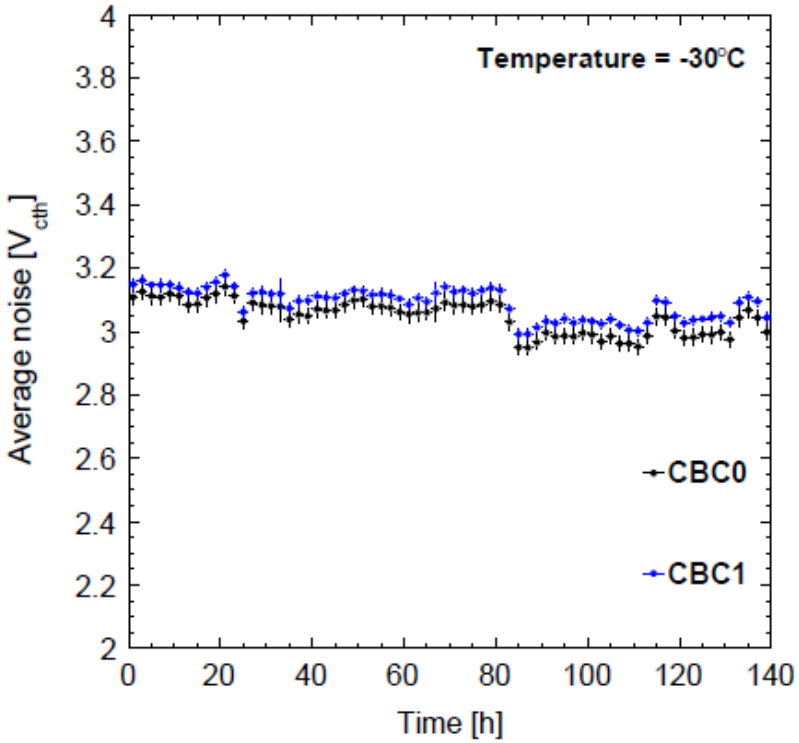

Sensor noise after time at -30C

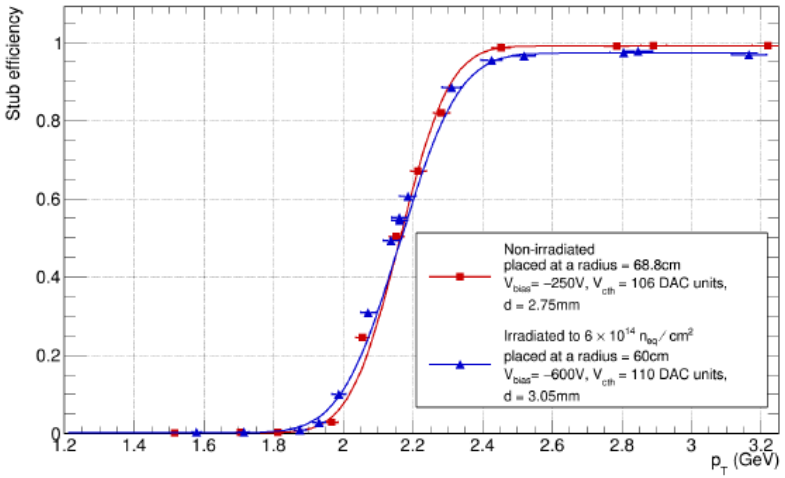

Figure 3.21: Stub reconstruction efficiency for a non-irradiated (red) and an irradiated (blue) 2S mini-module. The mini-module was irradiated to a fluence of $6 \times 10^{14}\,n_{eq}/cm^2$. The variable V_{cth} refers to the threshold setting, while d is the sensor spacing. The thresholds used correspond to about 4900 and 3500 electrons for the unirradiated and irradiated module, respectively. Radii of 69 cm and 60 cm were used for the calculation of the p_T from the tilt angle of the non-irradiated and irradiated module, respectively (Section 9.2.5.3). The different radii compensate for the fact that the modules had different sensor spacing but were operated with the same stub acceptance window.

HIT OCCUPANCY

Figure 6.3: Hit occupancy, defined as the fraction of channels containing a digitized hit, as a function of η for all layers and double-discs of the Inner Tracker (top) and Outer Tracker (bottom), for $t\bar{t}$ events with a pileup of 200 events. For the Outer Tracker, the occupancies in strip sensors and macro-pixel sensors are shown by filled and unfilled markers, respectively.

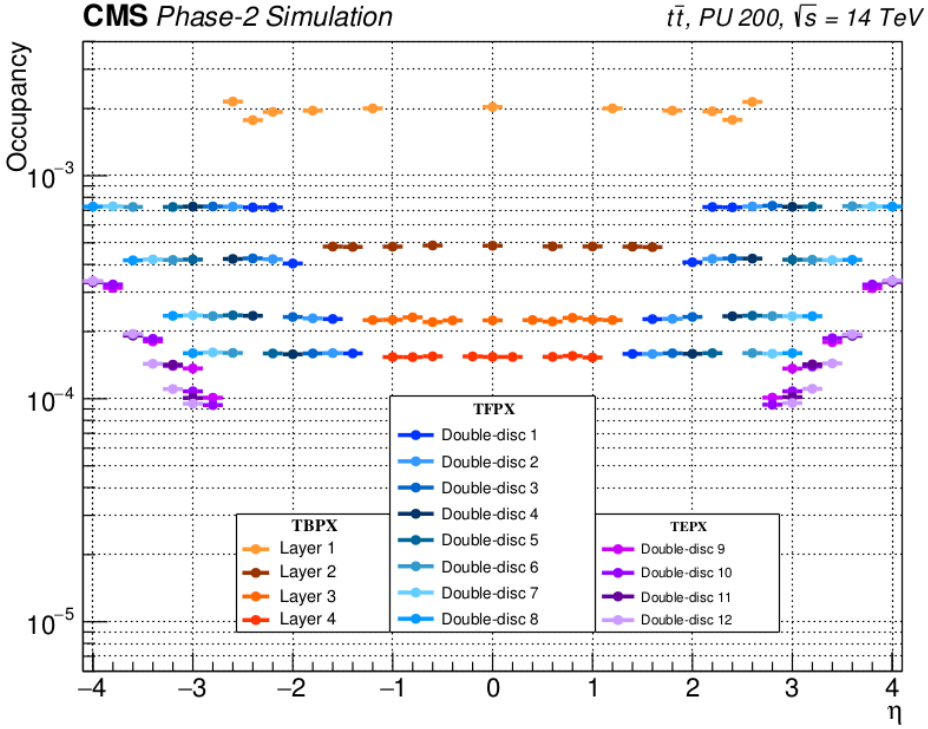

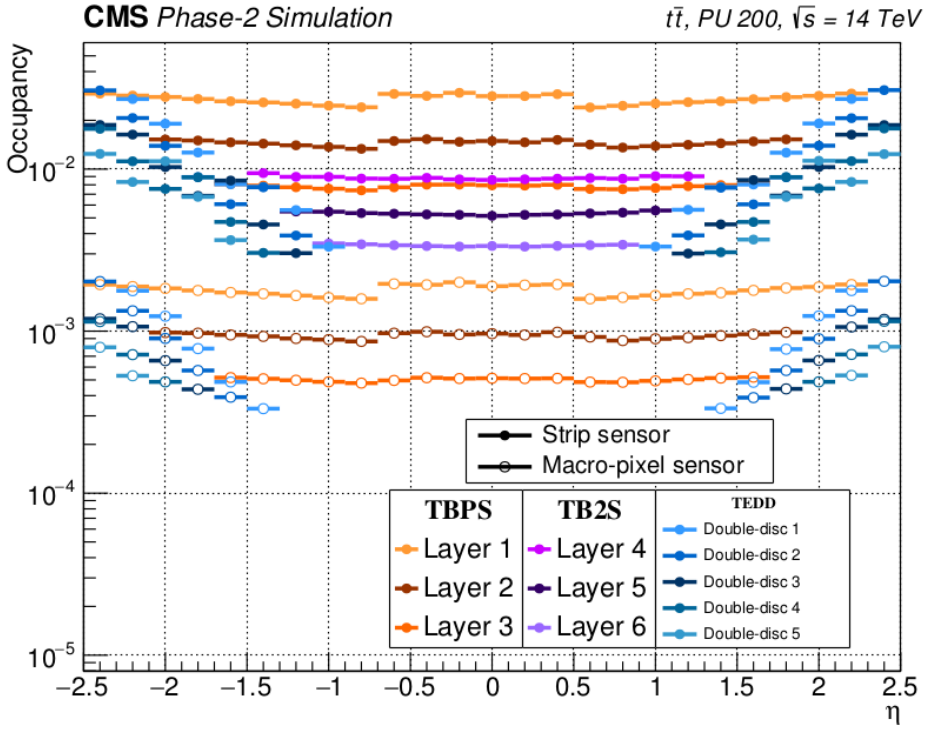

TRACKING

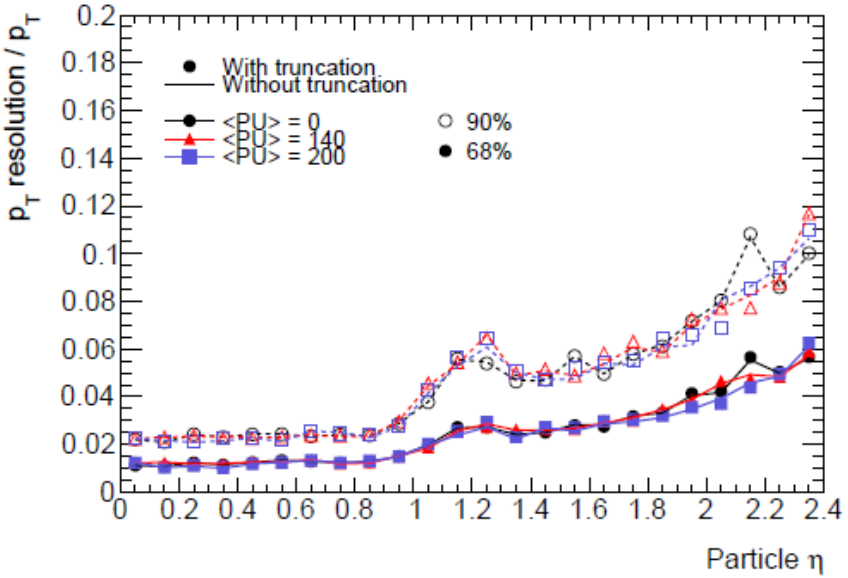

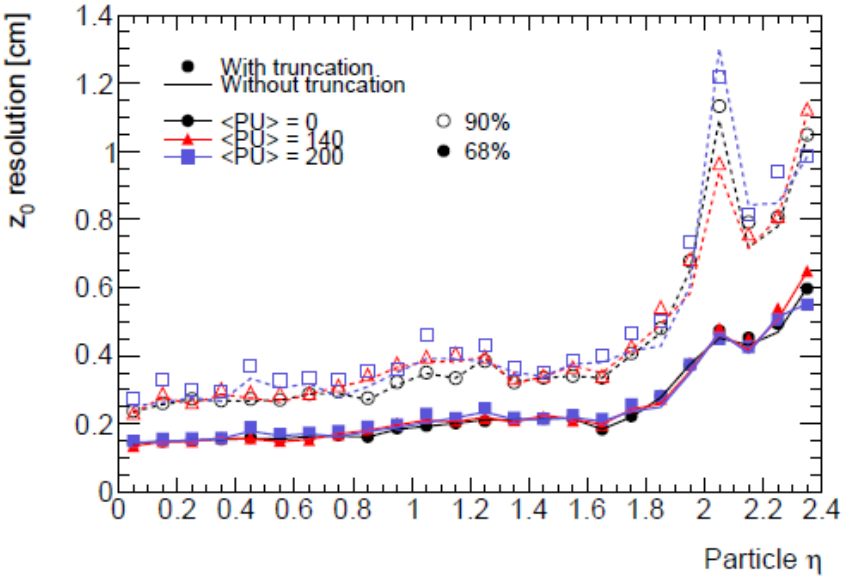

Figure 6.8: Relative p_T resolution (left) and z_0 resolution (right) versus pseudorapidity for muons in $t\bar{t}$ events with zero (black dots), 140 (red triangles), and 200 (blue squares) pileup events on average. Results are shown for scenarios in which truncation effects are (markers) or are not (lines) considered in the emulation of L1 track processing. The resolutions correspond to intervals in the track parameter distributions that encompass 68% (filled markers and solid lines) or 90% (open markers and dashed lines) of all tracks with $p_T > 3\,\text{GeV}$.

TRACKING

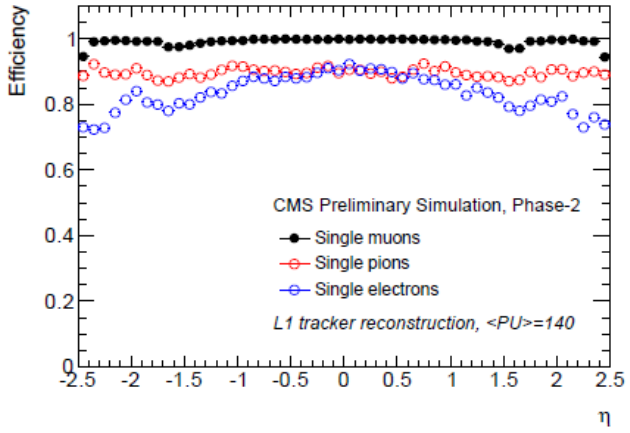

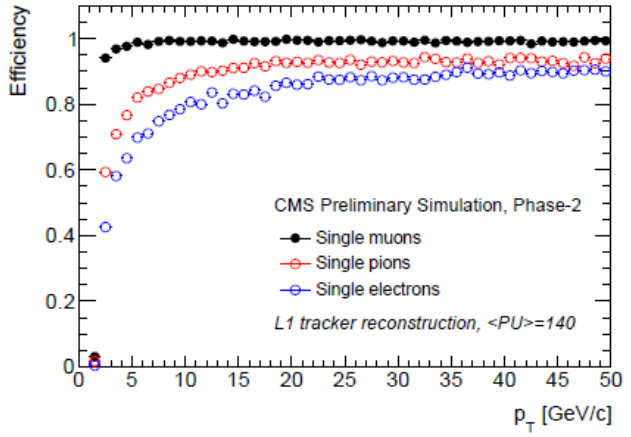

Figure 2.25: Efficiency for L1 track reconstruction as a function of η (left) and p_T (right) for muons, pions, and electrons.

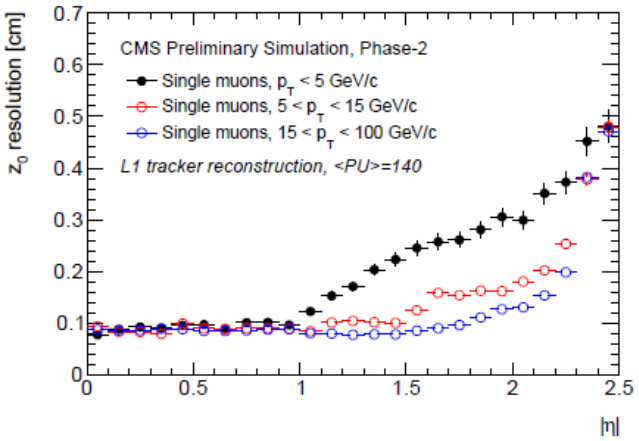

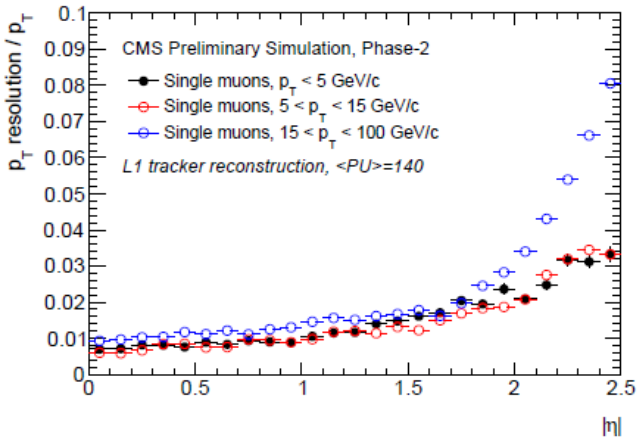

Figure 2.26: Resolution in z_0, and relative resolution in p_T for the L1 track reconstruction of single muons as function of η for different p_T ranges.

TRACKING

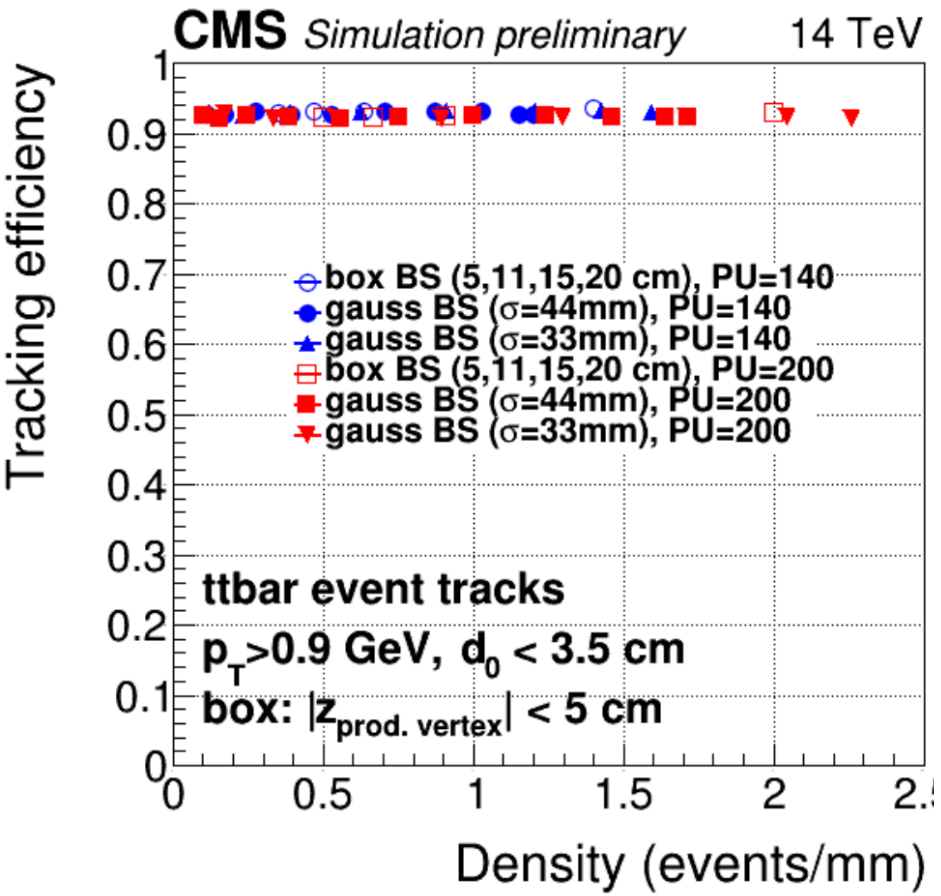
CMS Simulation preliminary
14 TeV
Tracking efficiency
box BS (5,11,15,20 cm), PU=140
gauss BS (σ=44mm), PU=140
gauss BS (σ=33mm), PU=140
box BS (5,11,15,20 cm), PU=200
gauss BS (σ=44mm), PU=200
gauss BS (σ=33mm), PU=200
ttbar event tracks
p_T>0.9 GeV, d_0 < 3.5 cm
box: |z_prod. vertex| < 5 cm
Density (events/mm)

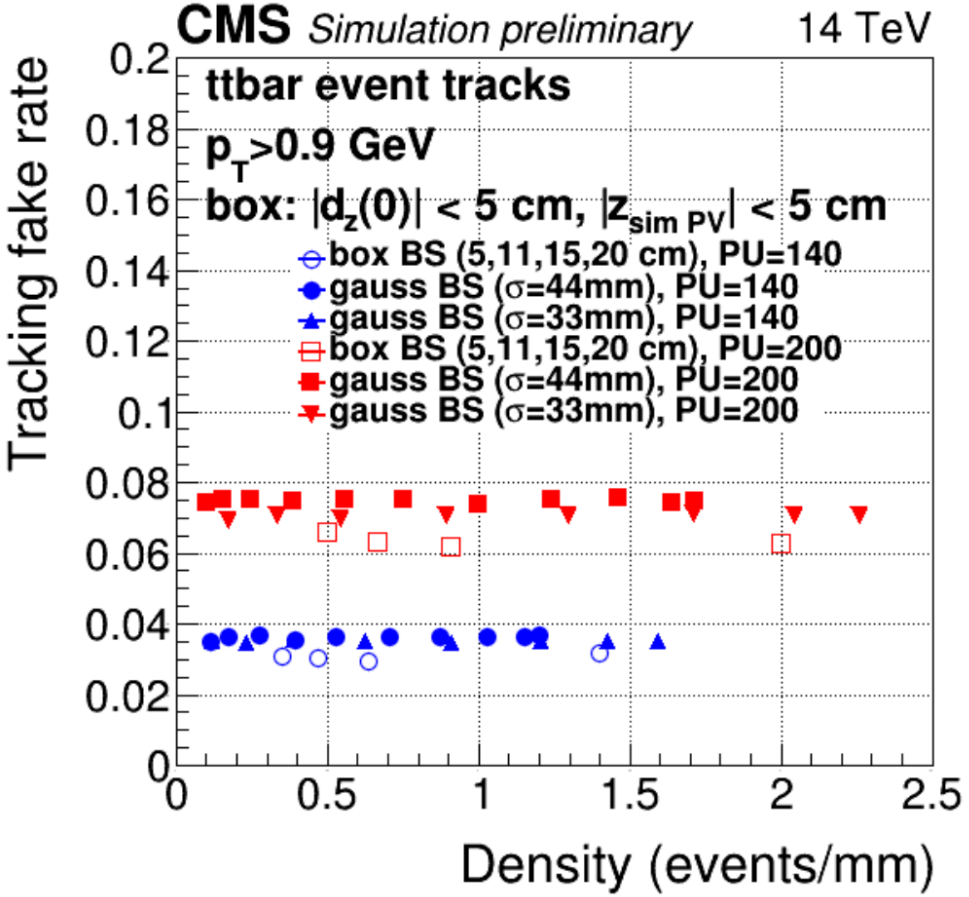
CMS Simulation preliminary
14 TeV
Tracking fake rate
ttbar event tracks
p_T>0.9 GeV
box: |d_z(0)| < 5 cm, |z_sim PV| < 5 cm
box BS (5,11,15,20 cm), PU=140
gauss BS (σ=44mm), PU=140
gauss BS (σ=33mm), PU=140
box BS (5,11,15,20 cm), PU=200
gauss BS (σ=44mm), PU=200
gauss BS (σ=33mm), PU=200
Density (events/mm)

CMS CALORIMETRY UPGRADES

- Electronics upgrades for barrel calorimeters to improve latency, add cluster timing capabilities, and lower the operating temperature
- **Radiation damage will cause large light losses in the endcaps**
  - AKA, endcaps will be dead by 1000/fb.
  - Complete replacement required with more robust technology
- High granularity silicon endcap calorimeter – 3D shower images

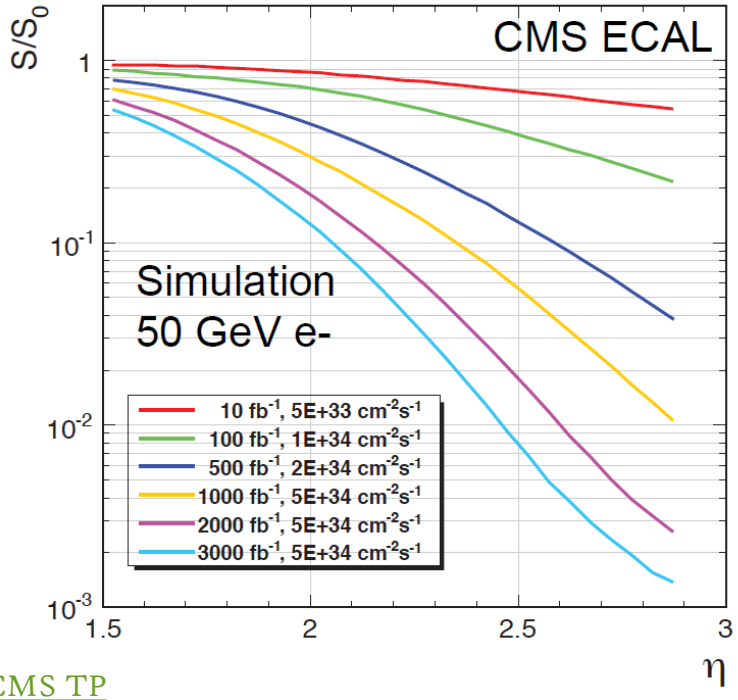

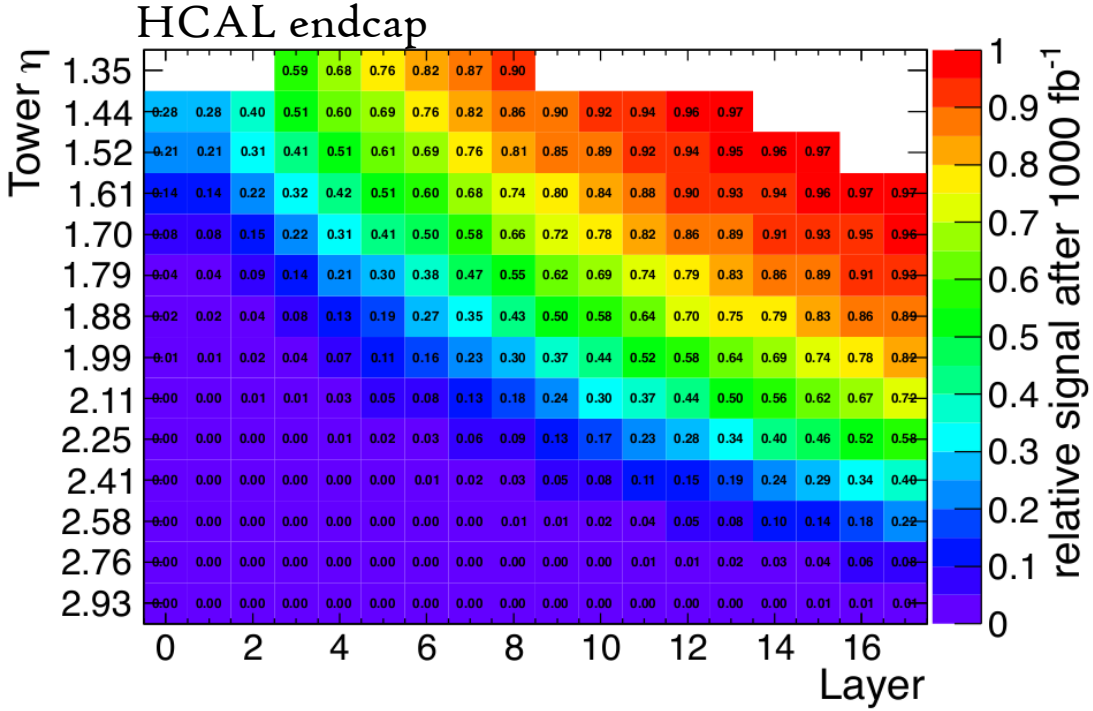

CMS TP

HCAL LIGHT LOSS

HCAL Barrel light loss

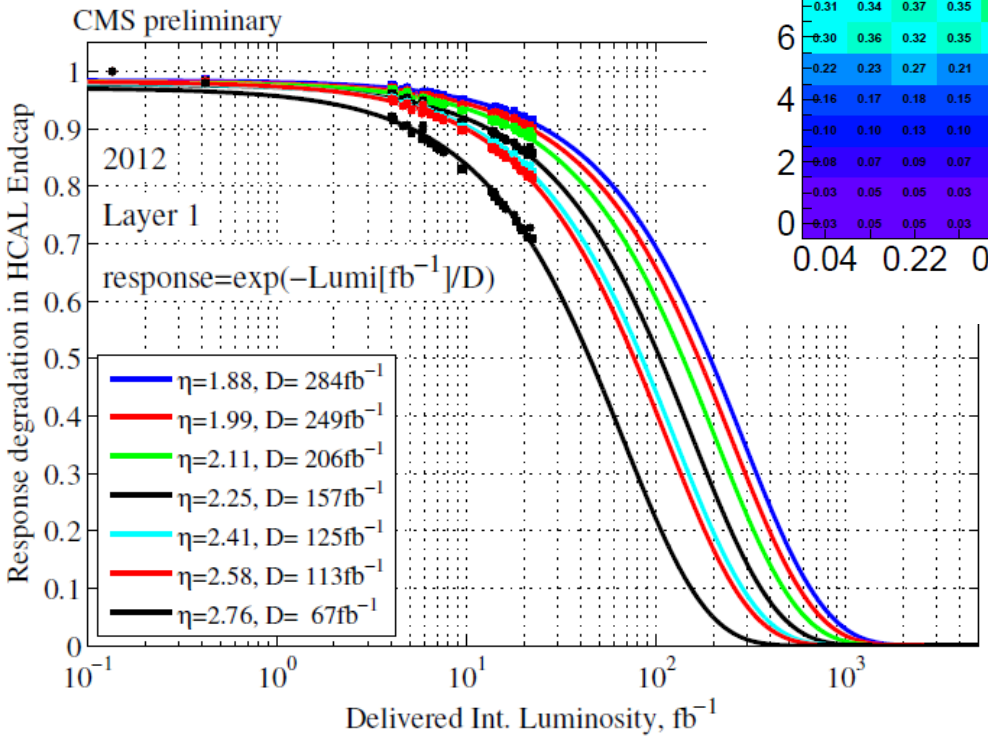

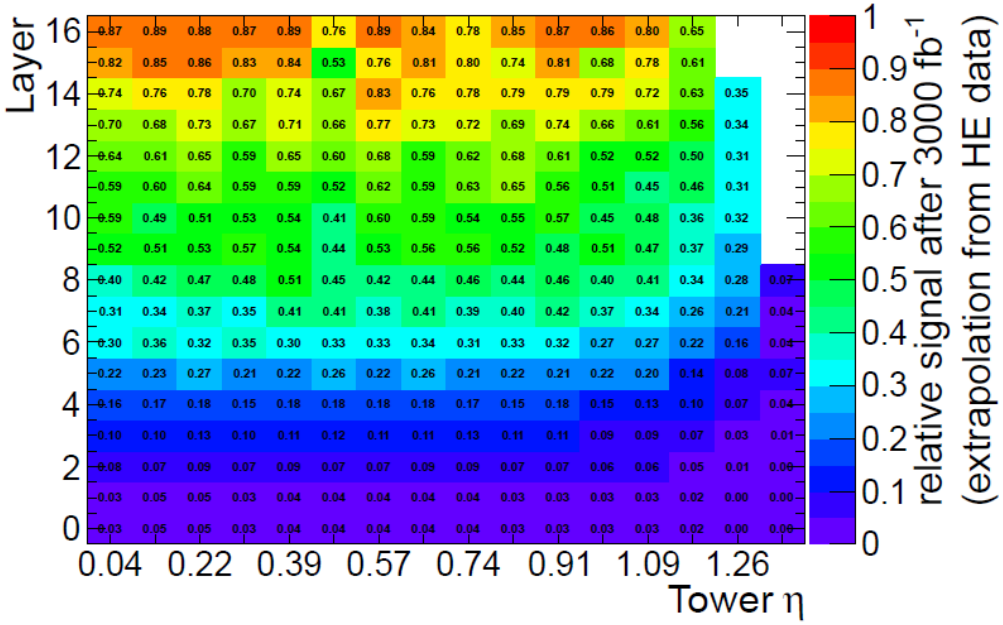

Figure 3.8: Fraction decrease of light signal from the first layer of HE as a function of accumulated luminosity for different values of the tile position (η), along with a fit to an exponential

ECAL TEMPERATURE

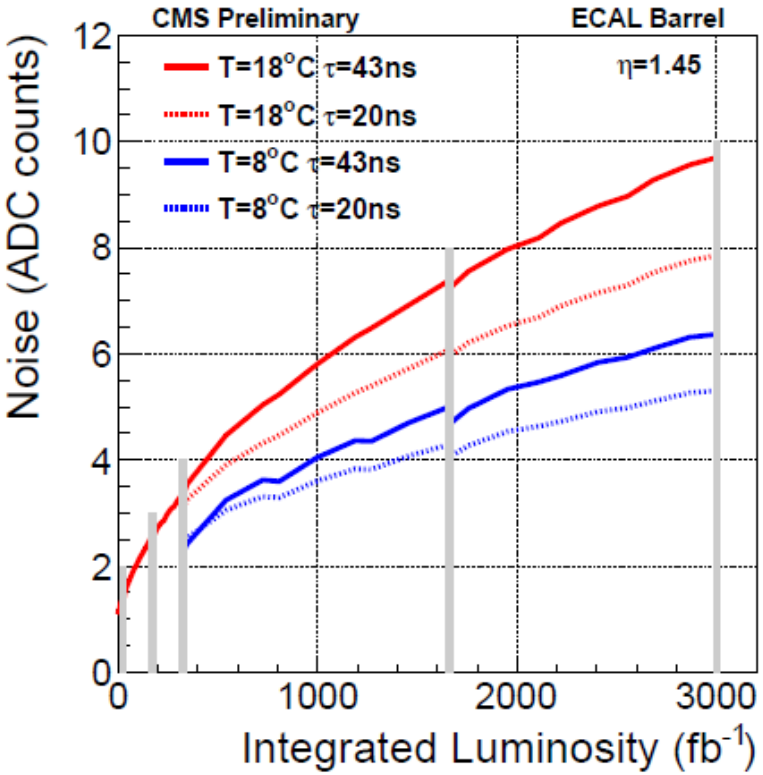

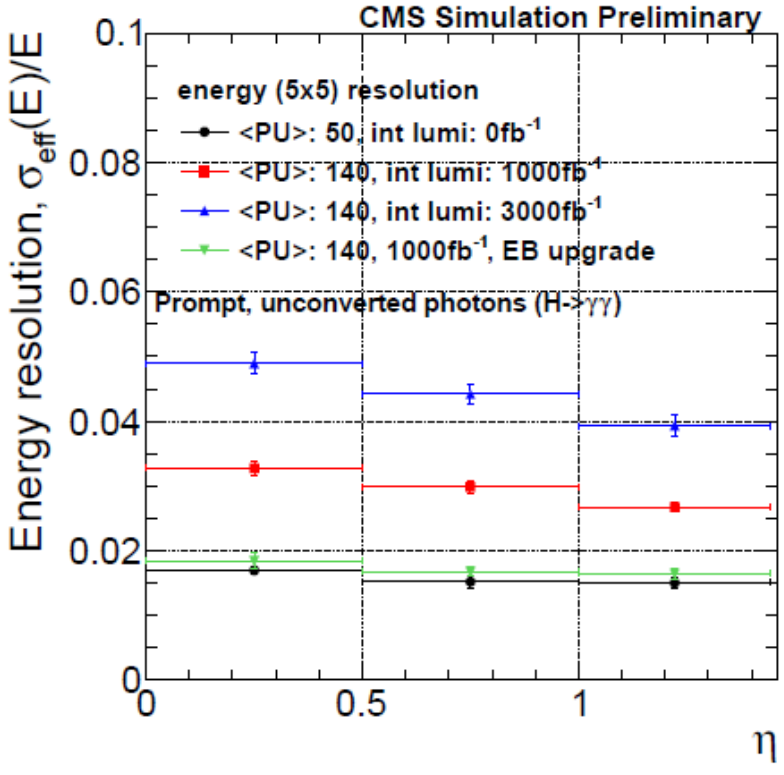

Figure 3.21: (Left) Expected noise level in the ECAL Barrel versus integrated luminosity at $\eta = 1.45$ if operating the detector at 18°C (red curves) or at 8°C (blue curve), with the present electronics (continuous line, shaping time τ =43 ns), or the upgraded electronics (dotted line, shaping time τ =20 ns). (Right) Energy resolution $\sigma_{eff}(E)/E$ for photons from the Higgs boson decay for different integrated luminosities and pileup, showing the resolution improvement provided by the upgrade to the barrel electromagnetic calorimeter (EB operated at 8°C and shaping time τ =20 ns).

HGCAL MODULE

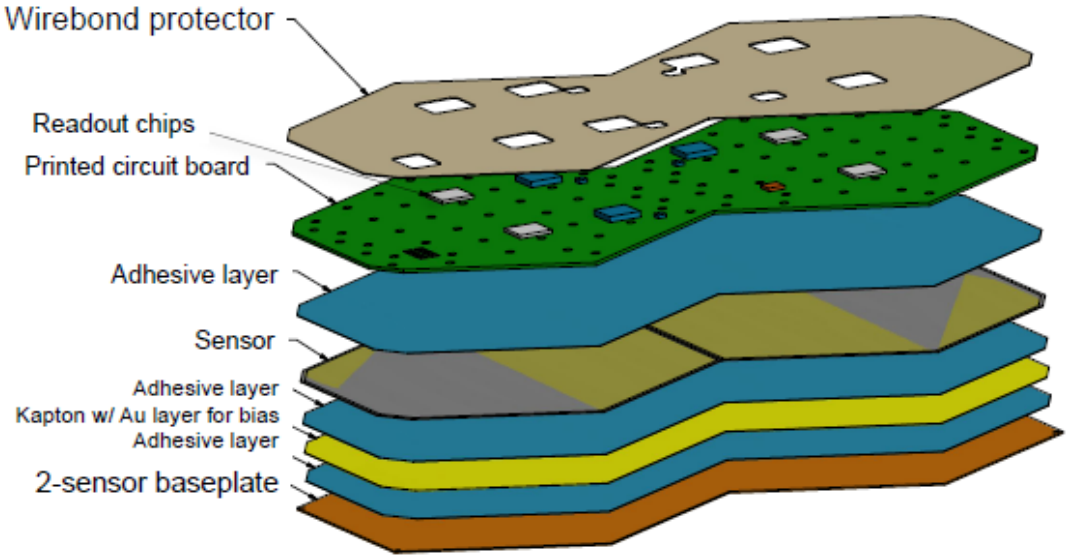

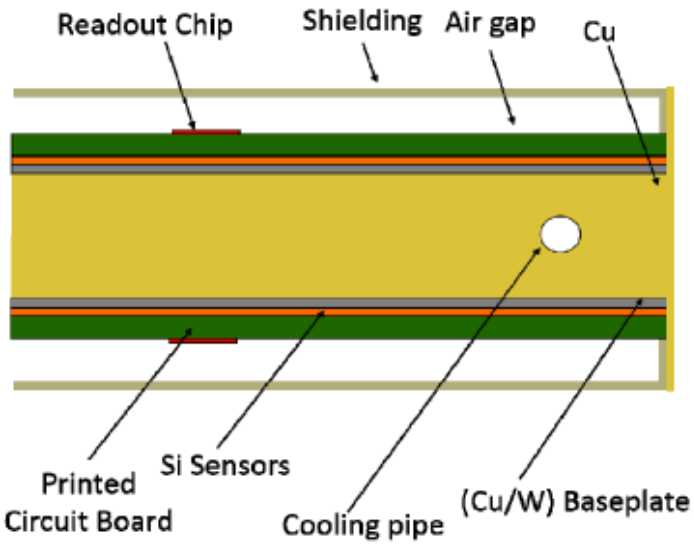

Figure 3.25: (Left) Module, consisting of printed circuit board, silicon sensors, and baseplate. (Right) Sketch of modules mounted either side of a copper and tungsten absorber/cooling plate, showing the longitudinal arrangement of a double layer.

JET RESPONSE

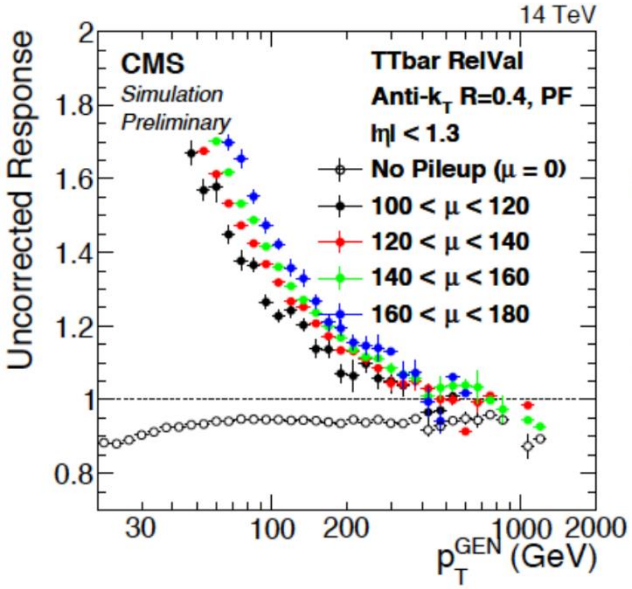

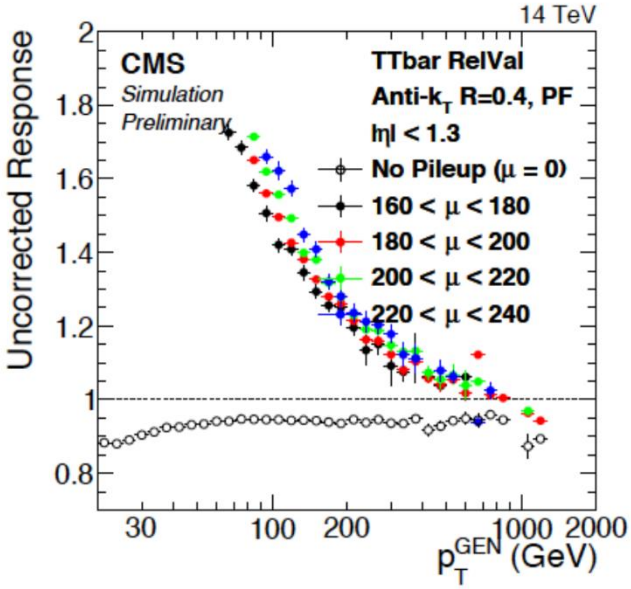

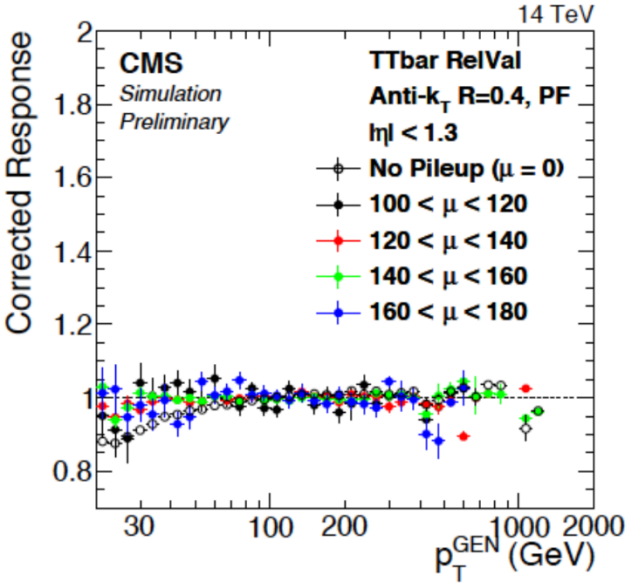

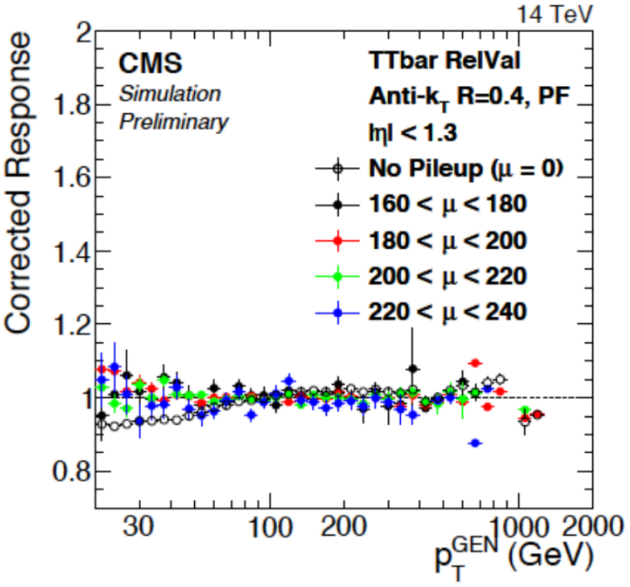

JET RESPONSE

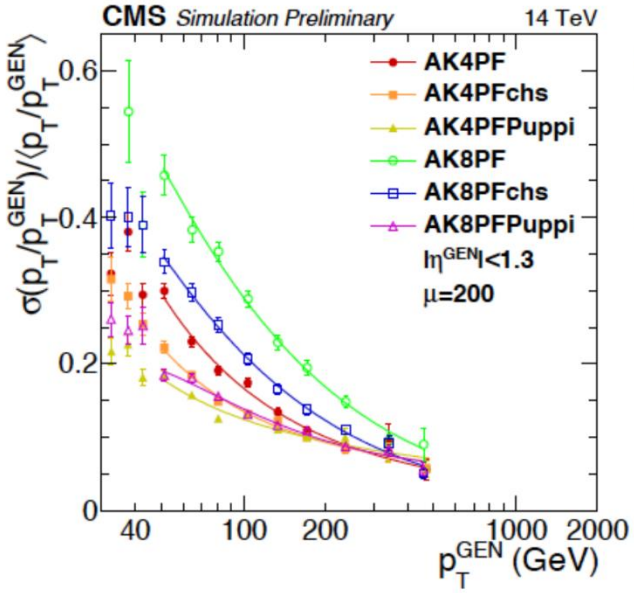

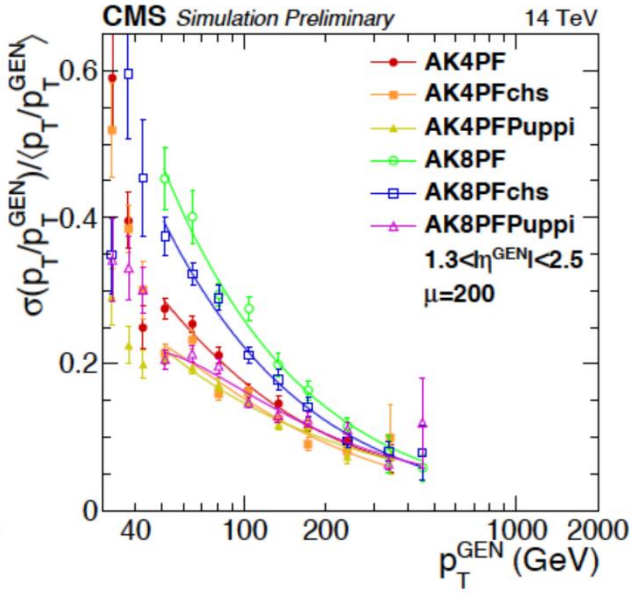

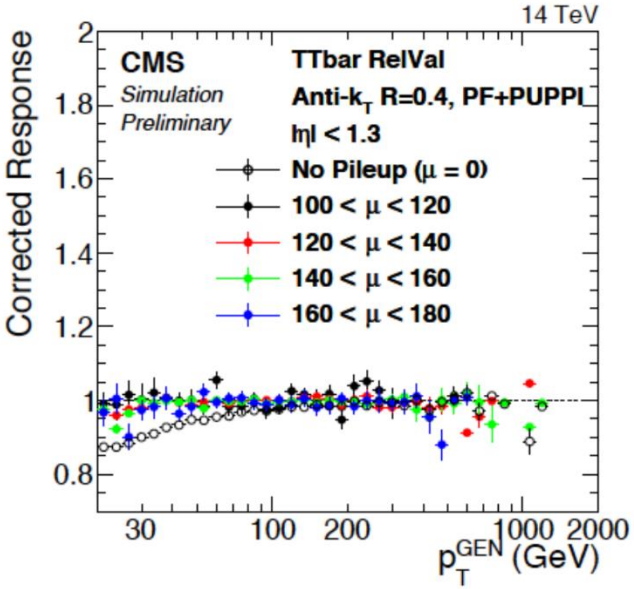

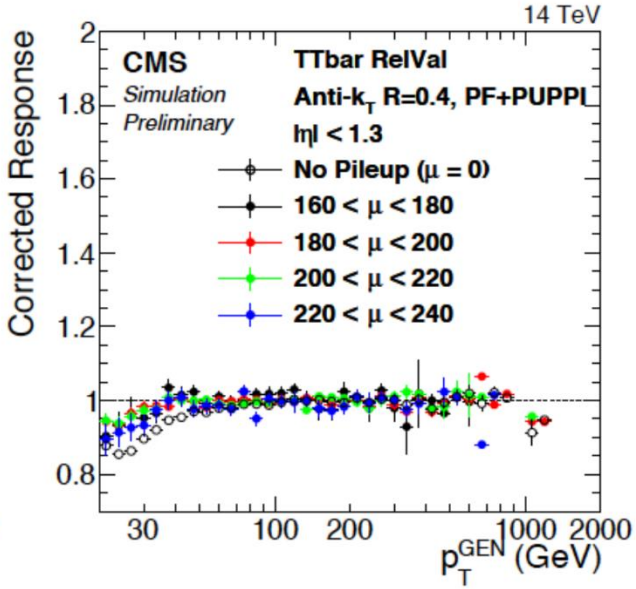

BTAGGING

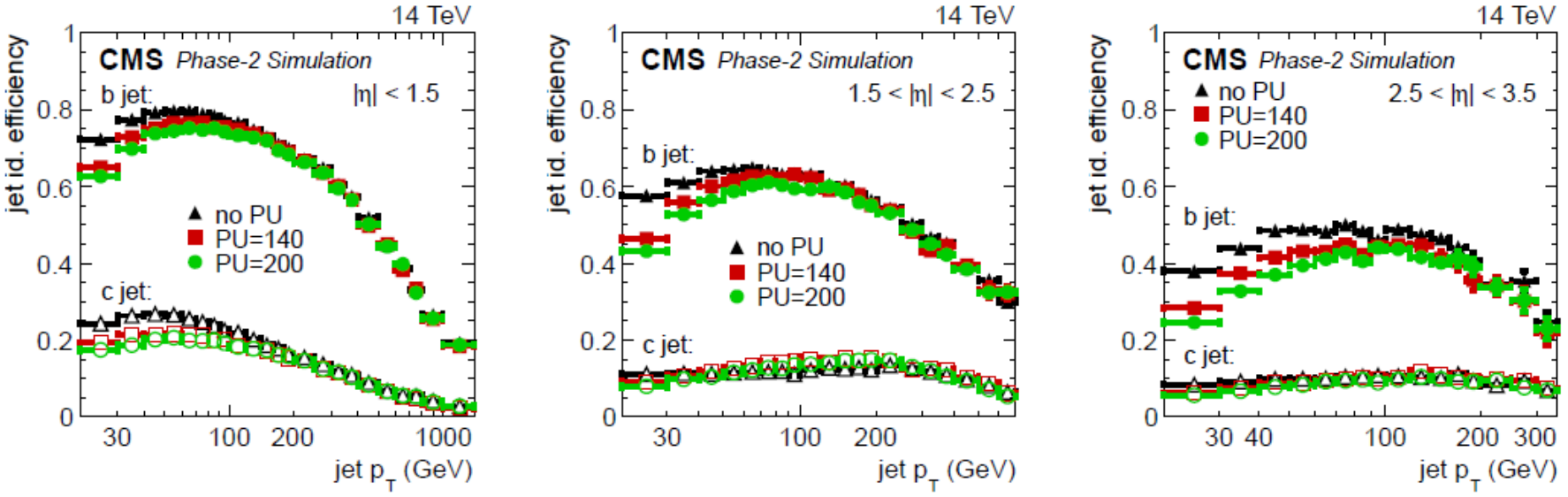

Figure 6.17: Tagging efficiencies for prompt b jets (filled symbols) and prompt c jets (open symbols) as a function of the jet p_T in simulated multi-jet events. The tagging efficiencies are evaluated for an average misidentification probability of 0.01 for light jets (udsg) and are shown for PU = 0 (black triangles), 140 (red squares), and 200 (green points). Three $|\eta|$ ranges are considered: 0–1.5 (left), 1.5–2.5 (centre), and 2.5–3.5 (right). The cMVAv2 and DeepCSV b tagging algorithms are used for jet $|\eta|$ within 0-1.5 and 1.5-3.5, respectively.

Z' AND W'

- CMS Z' → ttbar
  - Semileptonic and hadronic, both use boosted hadronic top tagging
  - **Could reach sensitivities to > 4 TeV Z' or KK Gluon** with top tagging improved to very low systematic uncertainties
- W' → tb
  - Leptonic top decay exploring the boosted b-jet + lepton system
  - **Expect sensitivity beyond current simulated bounds**

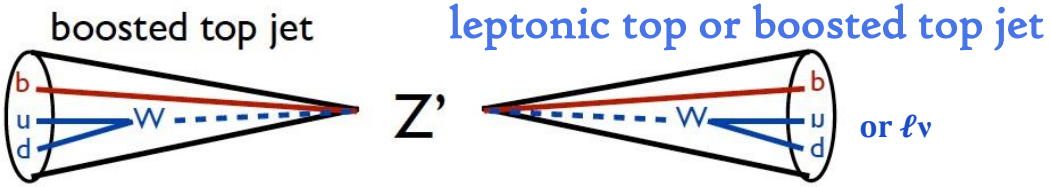

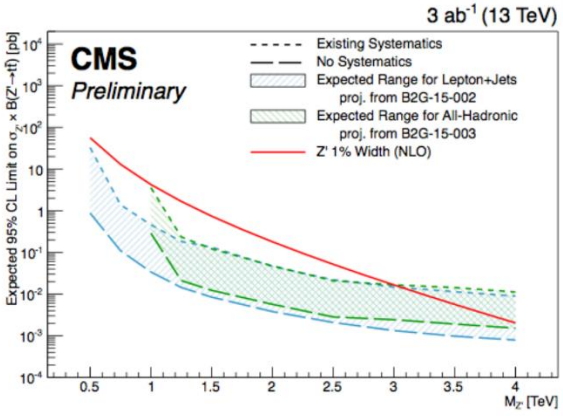

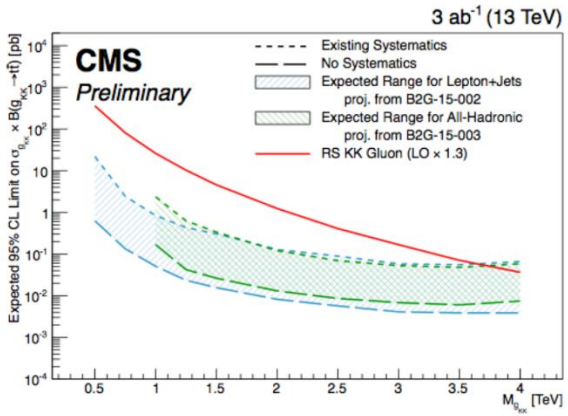

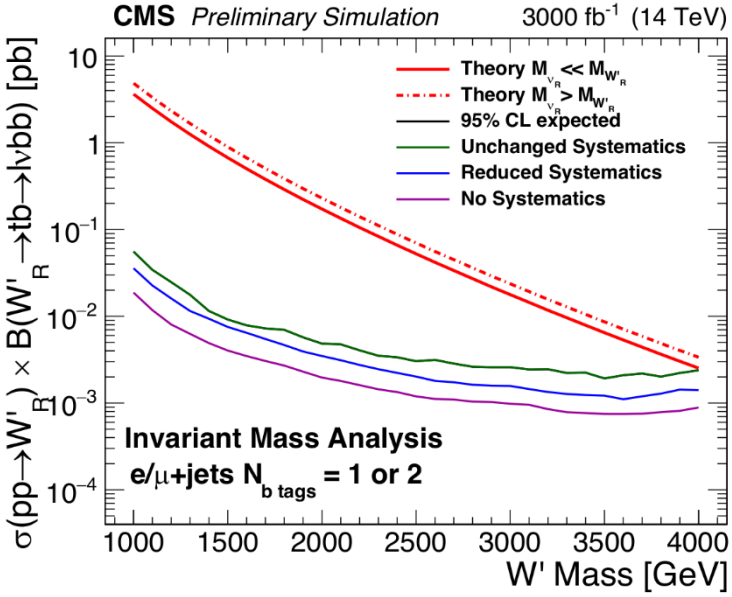

Z' AND W'

- ATLAS Z' → ttbar
  - Resolved and boosted top quark channels
  - **Also reach sensitivities to > 4 TeV Z'** , one TeV gain for 10x lumi increase

resolved channel

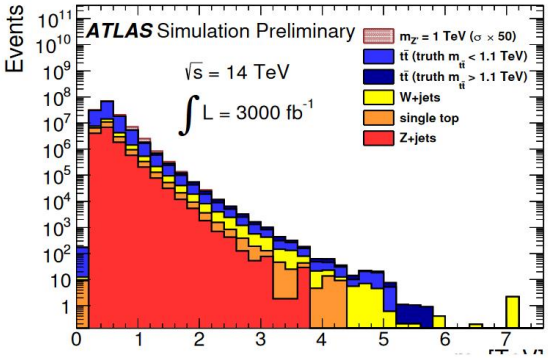

boosted channel

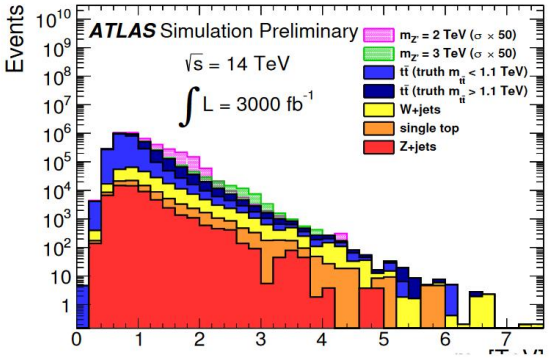

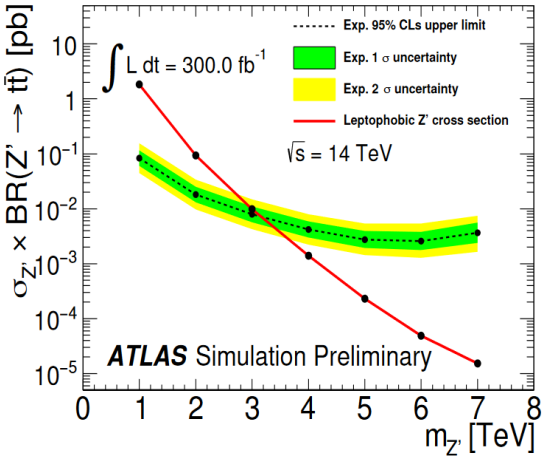

∫ ℒ after Run 3

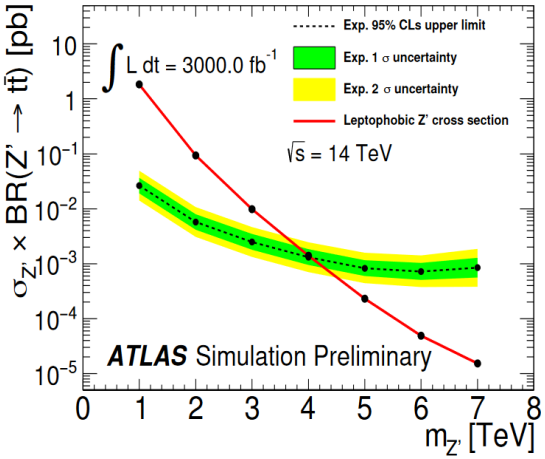

∫ ℒ after HL-LHC